EXPERIMENTAL STUDY OF PERSONALIZED AIR SYSTEM FOR THE REDUCTION OF POLLUTANT EXPOSURE

A thesis submitted in partial fulfillment of the requirements

for the Degree of Master of Philosophy

HUIGANG ZUO

Department of Building Services Engineering

The Hong Kong Polytechnic University

February, 2004

CERTIFICATE OF ORIGINALITY

I hereby declare that this thesis is my own work and that, to the best of my knowledge and belief, it reproduces no material previously published or written nor material which has been accepted for award of any other degree or diploma, except where due acknowledgement has been made in the text.

_____(signed)

_____Zuo Huigang_____(Name of student)

ABSTRACT

Abstract of thesis entitled

'Experimental Study of Personalized air system for the Reduction of Pollutant Exposure'

Submitted by Zuo Huigang

for the degree of Master Philosophy

at the Hong Kong polytechnic University

Current ASHRAE ventilation standard promulgates an outdoor intake around 10 l/s per person, with certain variations depending on building types. On the other hand, the metabolic human respiration rate for air is only around 0.1 l/s. In this thesis, we tested the concept of supplying ventilation in close proximity to nostrils and the facial area at much reduced airflow rate. A thermal manikin with a simulated lung is placed in a normal air-conditioned office. Fresh air supply is directed at the facial area of the manikin at flow rates raging from 0.1 to 4 l/s. The performance of personalized ventilation based on air movement in the vicinity of the occupant depends to a large extent on the supply air terminal device. Eight different air terminal devices were developed, tested and compared. CO_2 was used as a tracer gas, and injected into the supply air, and the CO_2 concentrations in the inhaled air, supplied air, and the ambient room air were measured, which were used to calculate two newly defined indices, i.e., the fresh air utilization efficiency η_u and the pollutant exposure reduction effectiveness η_{PER}. In the air supply flow rate range tested, the pollutant exposure reduction effectiveness increased with the increase of the airflow rate from the ATD to a

maximum value. Further increase of the airflow rate appears to have reduced impact on the pollutant exposure reduction effectiveness. The effects of the airflow around thermal manikin due to heat convection, the supply airflow rate, the cross-sectional area of air terminal devices and the geometry of air terminal devices were studied. Under both isothermal and non-isothermal conditions and an airflow rate below 4 L/s, a middle size circular air terminal device achieved the highest pollutant exposure reduction effectiveness 0.8. It is perceived that such a facial air supply method may have application potentials in those work places where occupants are sitting in a fixed position for prolonged period. An optimal air terminal device was recommended which has the best performance in improving an occupants' inhaled air quality.

ACKNOWLEDGEMENTS

I would like to express my gratitude to my advisor, Dr J.L Niu, for his constructive advice, continuous encouragement and enthusiasm during the course of this work.

I would also like to thank Dr. S.M Deng, my vice-advisor for his help of this work.

Finally, I would like to thank my wife, Ying Fan, and my parents for their love, patience, understanding and continuous moral support.

TABLE OF CONTENTS

LIST OF FIGURES

LIST OF TABLES

CHAPTER I: INTRODUCTION

1.1 The status of air conditioning and the advanced of Personalized air

Total-volume ventilation and air-conditioning of rooms is at present the method most used in practice. Mixing and displacement room air distribution are the main principles applied. Displacement ventilation has been shown to provide occupants with better air quality, especially in rooms with non-passive, heated contaminant sources (Brohus and Nielsen 1996). However, unlike mixing ventilation, the air temperature gradients in rooms with displacement ventilation are greatest at low air temperatures near the floor. High air velocities often exist near the floor as well. Thus, if not well designed, the risk of local discomfort due to draught and vertical temperature difference in rooms with displacement ventilation is high (Melikov and Nielsen 1989). Studies (Fang *et al.* 1998, 1999) show that the same air is perceived by people as being of poor quality at a high air temperature but of better quality at a low air temperature. In both rooms with mixing ventilation and those with displacement ventilation, the temperature of the air that will reach the breathing zone of occupants will be relatively high. The air quality perceived by the occupants will improve when more fresh air is supplied to the space. However, this will cause draught discomfort for some occupants.

In practice, rooms are used by occupants with different physiological and psychological response, clothing, activity, individual preferences to the air

temperature and movement, time response of the body to changes of the room temperature, etc. Thus, total-volume ventilation has limitations and is often unable to provide each occupant simultaneously with high thermal comfort and air quality. Often, occupants in rooms with mixing or displacement ventilation have to compromise between preferred thermal comfort and perceived air quality, simply because people have different preferred thermal comfort conditions. The compromise is different for each occupant and also differs in time. The disadvantage of the total-volume ventilation principle is that often room air movement is changed due to furniture rearrangement and this may increase occupants' complaints of draught and/or poor air quality.

Environmental conditions acceptable for most occupants in a room may be achieved by providing each occupant with the possibility to generate and control his/her own preferred local environment. Personalized air ventilation (PA), often referred as to task/ambient conditioning, aims to provide each occupant with personalized clean air direct to the breathing zone. Each occupant can control the environment at his/her workplace. Thus occupants' satisfaction and productivity can be increased as a result of improved air quality, thermal comfort and control over the environment. Energy use may be lowered, depending on system design and operation.

1.2 The primary importance for occupants' perceived air quality

In a calm, comfortable environment, upward free convection movement exists around the human body due to the temperature difference between the room air and the surface of the clothing and of the skin of bare body parts. The free convection flow becomes weak when the temperature difference is small. The airflow is slow and laminar with a thin boundary layer at the lower body parts, and fast and turbulent with a thick boundary layer at the height of the head. The free convection movement will change the skin temperature due to convection heat transfer and will thus affect man's thermal sensation. The free convection flow transports air, which might be contaminated from the lower part of the space, upward to the breathing zone. It also carries the bioeffluents and vapour-emitted form the human body. Furthermore, occupants' breathing generates an air movement due to exhalation. The interaction between the airflow from the personalized ventilation, the free convection flow around the body and the airflow of exhalation is of primary importance for occupants' thermal comfort and perceived air quality. The interaction is influenced by the strength of the free convection flow and the thickness of its boundary layer, the characteristics of the invading flow generated by the personalized ventilation (mean velocity, velocity profile, turbulence intensity, direction, temperature, etc.), the posture, the shape and area of the occupant's body exposed to the invading flow, the clothing design, etc.

The effect of thermal plume around human body, the effect of exhaled and inhaled airflow, the effect of personalized ventilation airflow and their interaction should be studied in this thesis.

1.3 The optimal air terminal device

The supply air terminal device is an essential part of any personalized ventilation system. It plays a major role in the distribution of personalized air around the human body and thus determines occupants' thermal comfort and perceived air quality.

A study on performance of different supply air terminal devices with regard to occupants' inhaled air quality was designed and performed. This paper compares the performance of ten supply air terminal devices in regard to the quality of air inhaled by the occupants and aims to find the optimal one.

1.4 Outline of the Thesis

This thesis consists of five chapters. In Chapter I, the actual air conditioning status and advances of personalized air system is introduced. The objectives of this research work are also covered. Then, a literature review of the personalized air system is presented in Chapter II. In chapter III, the experimental design details of personalized air system including supply air system, inhalation and exhalation system and thermal manikin are introduced. The results and summary

of this series of experiments are concluded in chapter IV. The conclusion and future works are presented in chapter V.

CHAPTER II: LITERATURE REVIEW

2.1 The status of Air conditioning system today and its problem

Air conditioning of building has been essential for economic development in areas with warm climates or warm summer. There are so numerous examples of the positive impact of air-conditioning, e.g. in eastern Asia and southern USA. Over the last 30 years, these areas have experienced a remarkably strong economic growth rate that would hardly have been possible without the widespread use of air-conditioning.

Today air-conditioning is used in many parts of the world, often in combination with heating and ventilation in HVAC systems. The image of such systems, however, is not always positive. The purpose of most systems is to provide thermal comfort and an acceptable indoor air quality for human occupants. But numerous field studies (Fisk et al 1993; Mendell 1993; Bluyssen et al 1996; Pejtersen et al 1999) have documented substantial rates of dissatisfaction with the indoor environment in many buildings. One of the main reasons is that the requirements of existing ventilation standards and guidelines (ASHRAE 1999; CEN 1998; ECA 1992) are quite low. The philosophy of these documents has been to establish an indoor air quality where less than a certain percentage (e.g. 15, 20 or 30%) of people are dissatisfied with the indoor air quality, while the rest may find the air barely acceptable. A similar thinking refers to the thermal

environment (EN ISO 1993). This philosophy behind the design of HVAC systems has led in practice to quite a number of dissatisfied persons (as predicted), while few seem to be ready to characterize the indoor environment as outstanding. At the same time numerous negative effects on human health are reported: many persons suffer from SBS symptoms (Fisk et al 1993; Mendell 1993; Bluyssen et al 1996) and a dramatic increase in cases of allergy and asthma have been related to poor indoor air quality (IAQ).

Based upon above review, Fanger (1999) pointed out that the indoor air quality is quite mediocre in many air-conditioned or mechanically ventilated buildings, even though existing standards may be met. A paradigm shift in the new century to search for excellence in the indoor environment is needed. The aim to provide indoor air that is perceived as fresh, pleasant and stimulating, with no negative effects on health, and a thermal environment perceived as comfortable by almost all occupants. In achieving this aim, due consideration must be given to energy efficiency and sustainability. Thermal comfort we do have a comprehensive database, while our knowledge on indoor air quality is still rather incomplete. This reflects the complexity of the interaction between indoor air quality and human comfort and health. But we do have some information on indoor air quality, as well as important new research results that will have a significant impact on the design of future air-conditioned or ventilated spaces for human occupants.

In practice, rooms are used by occupants with different physiological and psychological response, clothing, activity, individual preferences to the air

temperature and movement, time response of the body to changes of the room temperature, etc. Thus, total-volume ventilation has limitations and is often unable to provide each occupant simultaneously with high thermal comfort and air quality. Often, occupants in rooms with mixing or displacement ventilation have to compromise between preferred thermal comfort and perceived air quality, because some people are very sensitive to air movement while others are sensitive to the air quality. The compromise is different for each occupant and also differs in time. The disadvantage of the total-volume ventilation principle is that often room air movement is changed due to furniture rearrangement and this may increase occupants' complaints of draught and/or poor air quality.

2.2 The development of personalized air system

In many ventilated rooms the outdoor air supplied is of the order of magnitude of 10 l/s/person. Of this air, only 0.1 l/s/person, or 1%, is inhaled. The rest, i.e. 90% of the supplied air, is not used. And the 1% of the ventilation air being inhaled by human occupants is not even clean. It is polluted in the space by bioeffluents, emissions from building materials and sometimes even by environmental tobacco smoke before it is inhaled.

According to normal engineering practice, full mixing of clean air and pollutants seems to be an ideal. In the future, systems that supply rather small quantities of clean air close to the breathing zone of each individual may be proud of (Fanger 2001). The idea would be to serve to each occupant, clean air that is unpolluted by the pollution sources in the space. Small quantities of high-quality air will

directly serve to each individual rather than serving plenty of mediocre air throughout the space. Such "personalized air" (PA) should be provided so that the person inhales clean, cool and dry air from the core of the jet where the air is unmixed with polluted room air. In an office, the PA may come from an outlet next to the PC on the desk as shown on Figure 2.2. It is essential that the air is served "gently", i.e. has a low velocity and turbulence that do not cause draught (Fanger 1988).

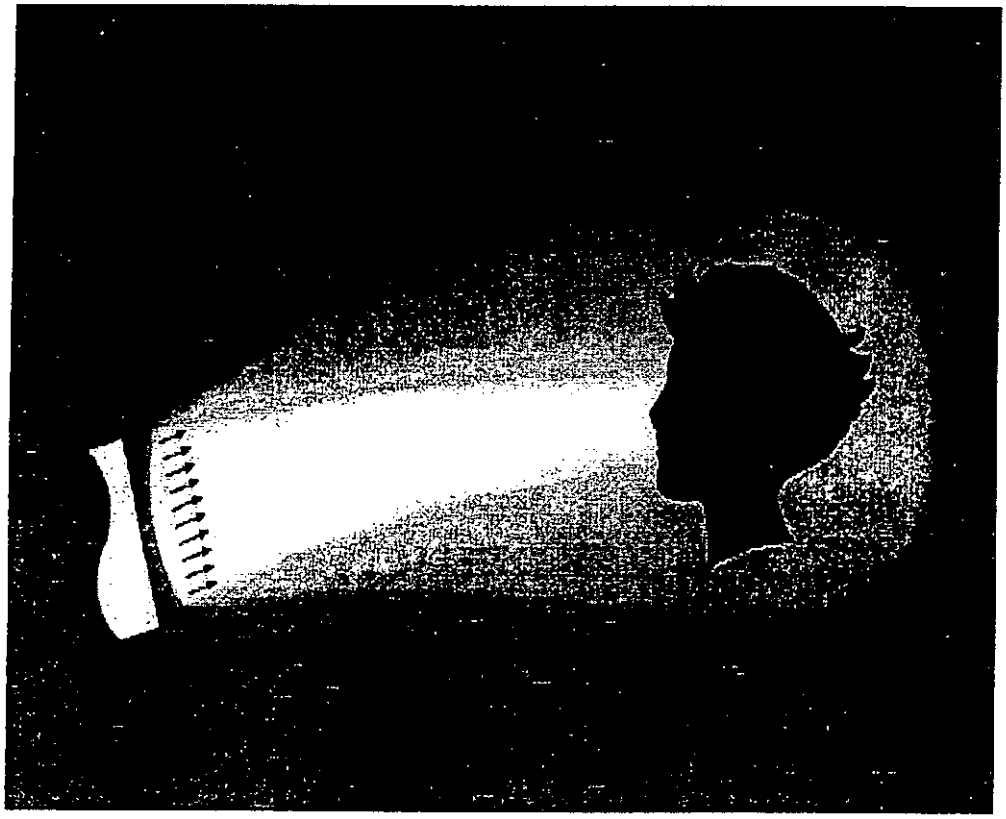

Figure 2.1. Personalized Air

Figure 2.2. PA comes from an outlet next to the PC on the desk (Fanger 2001)

Environmental conditions acceptable for most occupants in a room may be achieved by providing each occupant with the possibility to generate and control his/her own preferred local environment. Personalized air system (PA), often referred as to task/ambient conditioning, aims to provide each occupant with personalized clean air direct to the breathing zone. Each occupant can control the environment at his/her workplace. Thus occupants' satisfaction and productivity can be increased as a result of improved air quality, thermal comfort and control

over the environment. Energy use may be lowered for several reasons. The average room temperature may be raised, and the total outdoor air supply can be reduced.

2.3 The major role of the personalized air terminal device

In a calm, comfortable environment, upward free convection movement exists around the human body due to the temperature difference between the room air and the surface of the clothing and of the skin of bare body parts. The free convection flow becomes weak when the temperature difference is small. The airflow is slow and laminar with a thin boundary layer at the lower body parts, and fast and turbulent with a thick boundary layer at the height of the head. The free convection movement will change the skin temperature due to convection heat transfer and will thus affect man's thermal sensation. The free convection flow transports air, which might be contaminated from the lower part of the space, upward to the breathing zone. It also carries the bioeffluents and vapour-emitted form the human body. Furthermore, occupants' breathing generates an air movement due to exhalation and inhalation. The interaction between the airflow from the personalized air system, the free convection flow around the body and the airflow of exhalation is of primary importance for occupants' thermal comfort and perceived air quality. The interaction is influenced by the strength of the free convection flow and the thickness of its boundary layer, the characteristics of the invading flow generated by the personalized ventilation (mean velocity, velocity profile, turbulence intensity, direction, temperature, etc.),

the posture, the shape and area of the occupant's body exposed to the invading flow, the clothing design, etc.

The supply air terminal device is an essential part of any personalized air ventilation system. It plays a major role in the distribution of personalized air around the human body and thus determines occupants' thermal comfort and perceived air quality.

A study on performance of different supply air terminal devices in regard to occupants' thermal comfort and inhaled air quality was designed and performed. This paper compares the performance of eight supply air terminal devices with regard to the quality of air inhaled by the occupants.

2.4 The evaluation indices

Several indices have been used to assess the air movement efficiency around occupants: Air Change Effectiveness (ACE, CER standard 1752), Ventilation Effectiveness or Pollutant Removal Efficiency ε_v (Brohus and Nielsen, 1996) and Personal Exposure Effectiveness ε_p (Melikov 2001).

2.4.1 Air Change Effectiveness (ACE)

$$ACE = \frac{Average\_Air\_Age_{room}}{Average\_Air\_Age_{breathing\_zone}} \qquad (2\text{-}1)$$

Which if ACE=1 means the supply ventilation and exhaust ventilation has perfect mixing; ACE<1 means there's a short circuit (compared with perfect mixing ventilation) between supply inlet and exhaust outlet; ACE>1 means there's a short circuit (compared with perfect mixing ventilation) between supply inlet and breathing zone. This index is used to quantify the flow pattern, which is independent of the location of pollution sources.

2.4.2 Ventilation Effectiveness or Pollutant Removal Efficiency (ε_v)

$$\varepsilon_v = \frac{C_e - C_s}{C_i - C_s} \tag{2-2}$$

where C_e is pollutant concentration in ambient room air without supply air

C_s is pollutant concentration in supply air

C_i is pollutant concentration in inhaled air

ε_v =1 means the supply air and ambient room air was perfect mixing; ε_v <1 means the mixing of supply air and ambient room air was worse than perfect mixing; ε_v >1 means the mixing of supply air and ambient room air was better than perfect mixing. This index is used to quantify the concentration relationship between inhaled air and ambient room air (the latter comes from mass conservation). It is used to compare the eventual effect of different ventilation systems on breathing zone. It's a function of both flow pattern and pollution source location.

2.4.3 Personal Exposure Effectiveness (PEE)

$$\varepsilon_p = \frac{C_e - C_i}{C_e - C_s} \tag{2-3}$$

where C_e is pollutant concentration in the ambient room air without supply air

C_s is pollutant concentration in supply air

C_i is pollutant concentration in inhaled air

Which if ε_p=0 means the supply air and ambient room air was perfect mixing; ε_p=1 means inhaled air contains only personalized air. The parameter ε_p expressed as the percentage of personalized air in inhaled air..

The index ACE has to be obtained by tracer gas measurement. There are three methods to obtain the value of air age: Pulse method ($\tau_p = \frac{\int_0^\infty \tau C_p(\tau) d\tau}{\int_0^\infty C_p(\tau) d\tau}$), Decay method ($\tau_p = \frac{\int_0^\infty C_p(\tau) d\tau}{C_p(0)}$) and Rise methods ($\tau_p = \int_0^\infty [1 - \frac{C_p(\tau)}{C_p(\infty)}] d\tau$) methods.

This is a transient measurement, which needs long time to finish. In practice, ACE can be derived by CFD simulation.

Similarly, ε_p and ε_v can be directly derived by tracer gas measurement or by CFD simulation. The relationship between ε_v and ε_p can be expressed by:

$$\varepsilon_v = \frac{1}{1 - \varepsilon_p} \quad \text{or} \quad \varepsilon_p = 1 - \frac{1}{\varepsilon_v}$$

For the personalized ventilation, Personal Exposure Effectiveness (PEE) was used to assess the performance of the tested air terminal devices (Melikov, 2001). However, no any single index could evaluate the thermal comfort, perceived air quality and energy saving, some new indices should be introduced or developed to achieve these aims.

2.4.4 Two new evaluation indices

In our investigation, pollutant exposure reduction index η_{PER} is defined to express the personalized air pollutant exposure reduction effectiveness. If we assume that the pollutant in the personal supply air is zero, the index η_{PER} is defined as:

$$\eta_{PER} = \frac{(C_{a,P} - C_{L,P)}}{C_{a,P}} = 1 - \frac{C_{L,P}}{C_{a,P}} \tag{2-4}$$

where, $C_{a,P}$ is pollutant concentration in ambient room air, and $C_{L,P}$ is pollutant concentration in inhaled air. Numerically, η_{PER} is equal to the fraction of fresh air (i.e., the personalized supply air) in the inhaled air, which is in turn defined as ventilation coefficient η_f and can be calculated from the measured tracer gas CO_2 concentrations:

$$\eta_f = \frac{V_{F,L}}{V_L} = \frac{C_L - C_a}{C_F - C_a} \tag{2-5}$$

where, $V_{F,L}$ is the fresh air volume in the inhaled air, and V_L is the total inhaled air volume, C_F is CO_2 concentration of fresh supply air, C_a is CO_2 concentration of ambient room air, and C_L is CO_2 concentration of inhaled air. When an personal only inhaled the personal air that does not mix with any ambient room air, both η_{PER} and η_f are equal to 1. In this case, the inhaled air is free of any indoor air pollutants. In the other extreme, if the personalized air is already well mixed with ambient room air, we would have $C_L = C_a$, and both η_{PER} and η_f will be equal to 0, which means the personalized air system has no additional effects as compared with mixed ventilation system.

Although both η_{PER} and η_f numerically equal to the PEE as defined by Melikov (2001), their physical meanings are more clear, and η_{PER} can be used to compare the IAQ benefits and energy saving potentials of personalized air supply in comparison with the whole-space air-conditioning system. This analysis is given in the Appendix. In conjunction, we define another new index, the fresh air utilization efficiency η_u that expresses the ratio of actual fresh air in the inhaled air to the supplied fresh air, and can be calculated as:

$$\eta_u = \eta_f * V_L / V_f \qquad (2\text{-}6)$$

where V_f is personal fresh air supply flow rate. η_{PER} and η_f better quantify the inhaled air quality, and η_u better quantifies the utilization efficiency of a ventilation system. (Zuo et.al 2002)

2.5 Air terminal device

As preliminary study by Melikov (2001), five different air terminal devices were developed and studied. The air terminal devices (ATD) that Arsen studied are schematically shown in Figure 4.1. The movable panel (MP) allows the direction of the personalized airflow in relation to the occupant to be changed within a wide range. The direction of the personalized airflow from the computer monitor panel (CMP), mounted on the monitor, can be changed on a vertical plane. The vertical desk grill (VDG) and the horizontal desk grill (HDG) mounted at the edge of the desk provide respectively a vertical and a horizontal flow of personalized air direct to the breathing zone of the occupant or against the occupant's body. During the tests, two of the ATD, namely CMP and VDG, were tested also in modified versions, CMP mod and VDG mod, having a 50% smaller cross-sectional area. These air terminal devices allow for changes of the airflow direction in specific range. The last air terminal device, the personal environments module (PEM) consists of two nozzles mounted at the two edges of the desk. They allow for changes of the direction of the personalized air in horizontal and vertical planes. This device described in detail in Tsuzuki et al. (1999) is available on the market and was provided by the manufacturer.

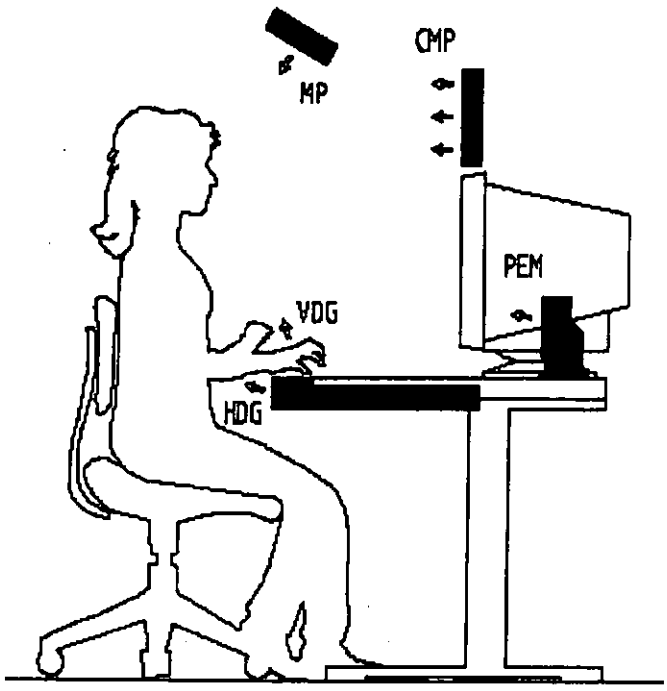

Figure 2.3 Air terminal devices studied: MP (Movable Panel), CMP (Computer Monitor Panel), VDG (Vertical Desk Grill), HDG (Horizontal Desk Grill), PEM (Personal Environments Module).

Personal exposure effectiveness (PEE) was used in his study to assess the performance of the test air terminal device. As his study indicate that under both isothermal and non-isothermal conditions and an airflow rate below 15L/s, the highest personal exposure effectiveness, 0.6, was achieve by a vertical desk grill (VDG) providing personalized air upward to the occupant's face. A movable panel (MP) allowing for a change of airflow direction in relation to the occupant had a high performance as well. According to Melikov (2001), the VDG and MP do not affect occupants' general thermal sensation significantly and are recommended to be used at comfortable room temperature.

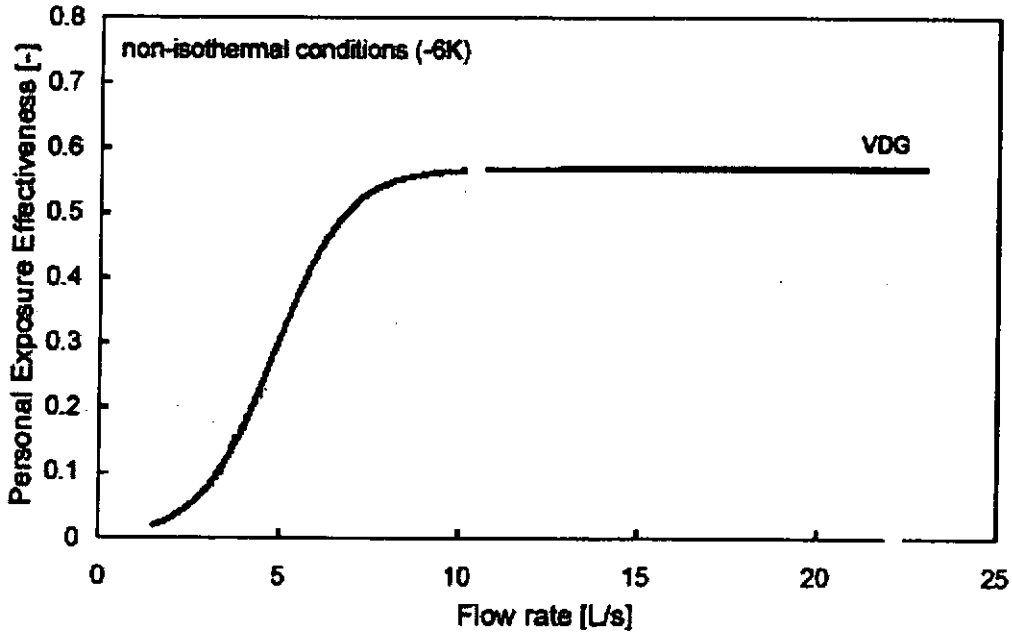

Figure 2.4 Personal exposure effectiveness as a function of the airflow rate from air terminal device VDG (Melikov 2001)

However, it can be noted that the required air supply rate to achieve a high PEE is still very close to the conventional ventilation system, and appears still far above the small human respiration volume.

CHAPTER III: PERSONALIZED AIR SYSTEM

In this chapter we will propose a new method to realize personalized air supply. We will use experimental methods to assess the performances of the method using the two indices, the pollutant exposure reduction effectiveness η_{per}, and fresh air utilization coefficient η_{fu}. The experimental design is detailed in this chapter.

3.1 Thermal Manikin

3.1.1 Introduction

Thermal manikins, originally developed to measure the thermal insulation of clothing, are heated dummies that simulate the heat transfer between humans and their thermal environment. A standing manikin for clothing studies was developed (Winslow and Herrington 1949) and became the model for many manikins, including standing copper manikin (Toda 1958). A seated thermal manikin (Kerslarke et al. 1965) and a male thermal manikin that can sit, stand, and even move (Madsen 1976a; 1976b) were developed later. It has been used to provide a comprehensive database for clothing insulation. Through a series of manikin measurements over the years, a comprehensive database of clothing insulation has been published (McCullout et al. 1985).

In 1977, a thermal manikin not only for clothing insulation measurements but also for the evaluation of thermal environments was been developed (Mihira et al. 1977). However, the relationship between measured heat loss and thermal sensation was unknown. The thermal manikin was been used for evaluations of the indoor environment (Olesen et al. 1979; Fanger et al. 1980, 1986). An aluminium thermal manikin also been used to evaluating thermal environments (Tanabe et al. 1989).

Recently, The manikin-derived EHT (equivalent homogeneous temperature) is proposed and demonstrated usefulness in evaluating strongly nonhomogeneous thermal environments in automobiles (Wyon et al. 1989). Wyon's manikin also has been used for the evaluation of heated spaces (Banhidi et al. 1991). Wyon's manikin is controlled to keep skin temperature constant. The thermal manikin also been used to predict discomfort due to displacement ventilation (Wyon and Sandberg 1990). The model is heated to body temperature and wears the actual clothing. Measurement of the heat loss from different part of such a model indicates the expected degree of thermal comfort for a person in the same position and wearing the same clothing as the measuring manikin.

Several thermal manikins have been developed today, some mainly for measurement of CLO-values (Olesen 1983) and others for evaluation of the thermal environment in buildings, but maybe even more in vehicles. Most of these manikins are divided up in more or less different, thermally independent zones in order to be able to evaluate the distribution of heat loss all over the body.

This is of interest for development of special protective clothing, but also for evaluation of new heating and ventilation systems.

Thirty years' experience with measurement of clothing insulation, and indoor thermal environment, is the background for developing this new thermal manikin (Madsen 1971; 1972; 1976; 1986; Tanabe 1994).

The topic was to develop an instrument that is easy to use, and at the same time an instrument, which simulate as accurately as possible, the thermal reaction of a human being on the indoor environment.

3.1.2 A breathing thermal manikin consisting of 20 body parts was used to simulate a human being

The manikin is a female model with 38 size 168cm height. The starting point has been an exhibition manikin made of fibreglass-armed polystyrene. This material gives a light and mechanical strong construction with, at the same time, a low thermal conductivity and a low thermal capacity. But these manikins are not made with normal human measures.

The manikin has movable junctions in neck, shoulder, hip and knee. The cut in the hip is made in a way so that the manikin is able both to stand and to be seated in natural position. In our investigation, the manikin was sat on an office chair.

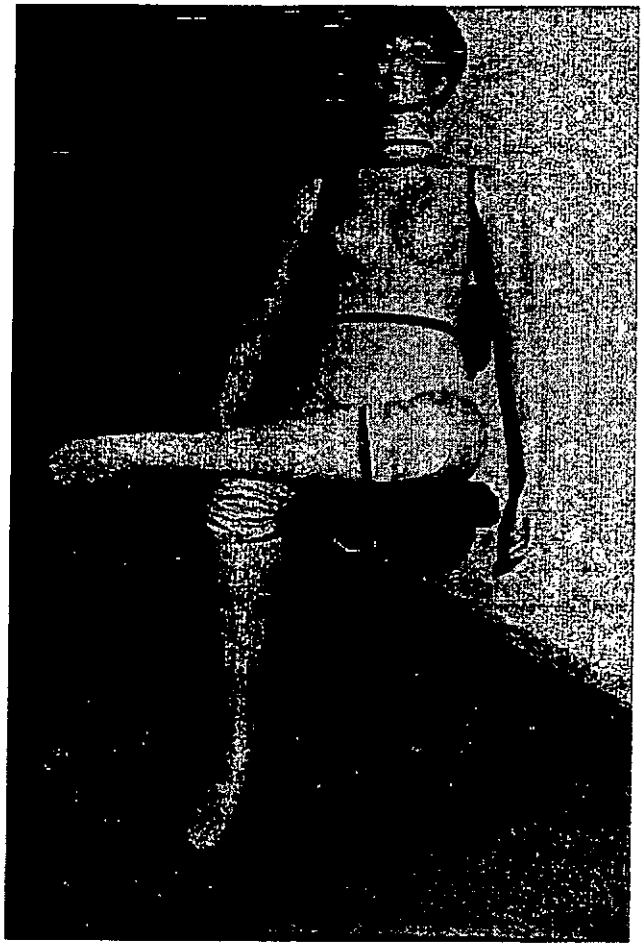

Figure 3.1 the seated thermal manikin

It is extremely important that the manikin is able to react on the thermal environment in the same way as a human being in the same situation and wearing the same clothing. To be able to do this, the manikin is divided in 20 thermally independent sections. Each part has its own computer control system.

3.1.3 The heating system of thermal manikin

Figure 3.2 the wiring of one hand is shown before the last protective layer is added on top of the wiring

The manikin consists of 4-mm fibreglass-armed polyester shell wound with nickel wire of 0.3-mm diameter at a maximum spacing of 2 mm. The wiring is covered by a 0.1-mm to 1.0-mm protective shield. The heating element is placed close to the surface to give the manikin a very small time constant (less than five minutes) compared to other thermal manikins. The time constant is further reduced by the fact that the same nickel wire is used sequentially both for heating the manikin and for measuring and controlling the skin temperature. For the nude manikin with a heat loss of 100 W/m^2, the difference in surface temperature between the hottest point directly above a wire and the coldest point midway

between two wires was measured to be less than 0.5 ℃ using infrared thermo vision equipment.

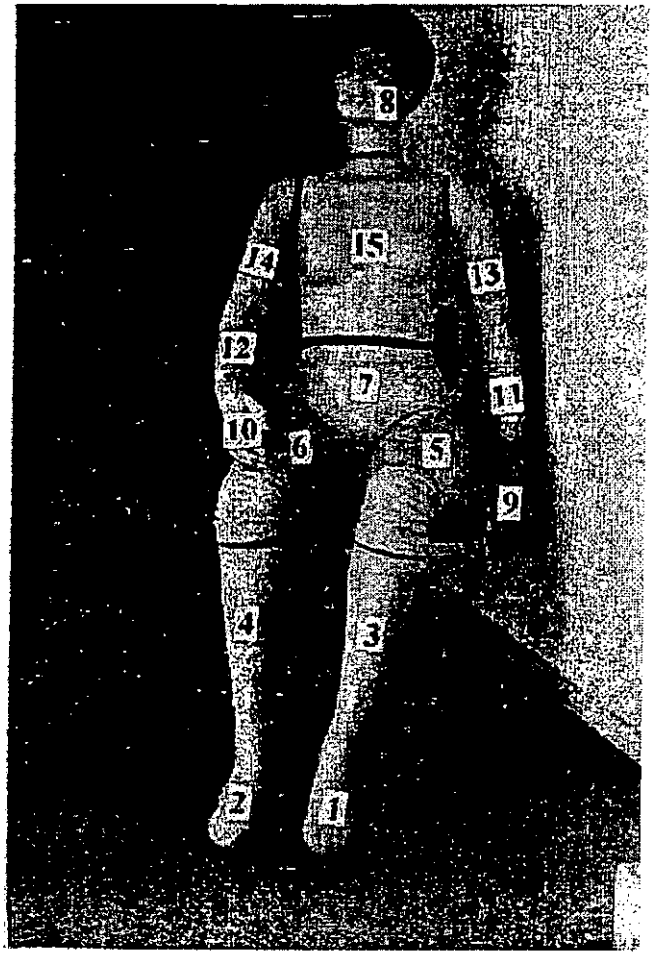

Figure 3.3 the manikin is divided in independent sections, each with its own breathing and computer control system

Figure 3.3 is picture of the thermal manikin.. Each part is separately controlled and measured by a laptop computer outside the manikin. Data are output from the control computer for storage and spreadsheet analysis (As shown on Figure 3.4).

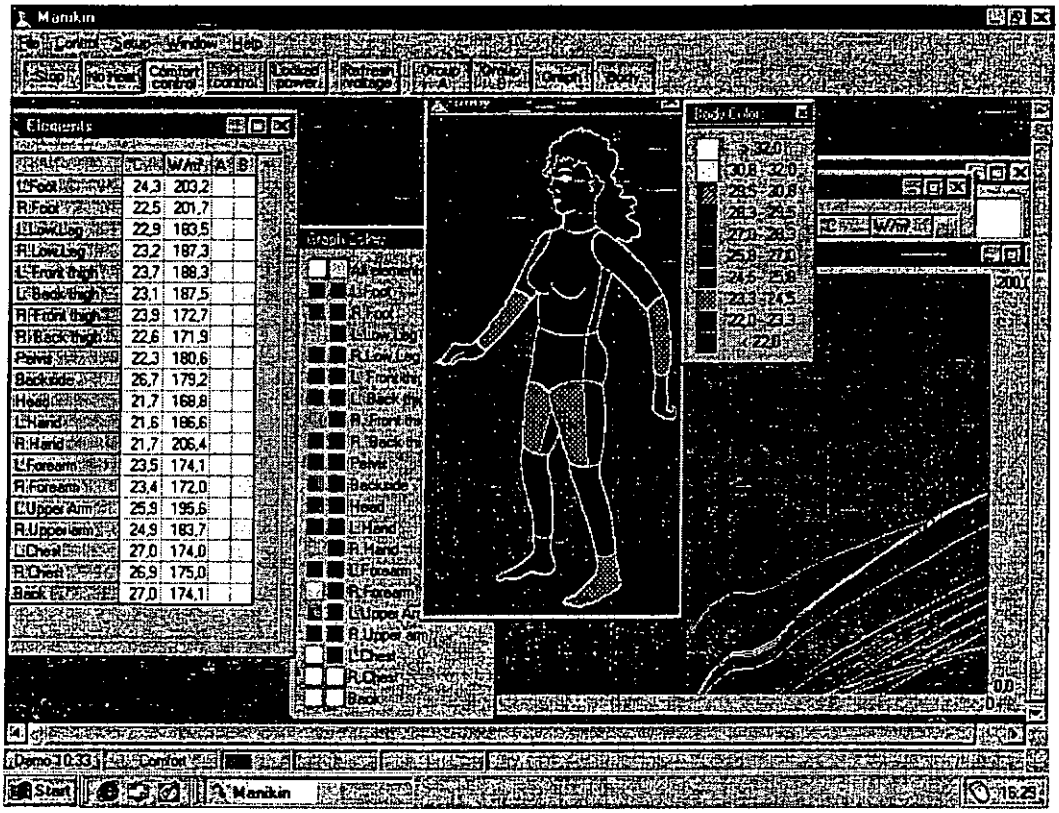

Figure 3.4. Software of data output and control system

3.1.3. Manikin Control Principles

There are two major control methods used for manikins. One is to keep the heater temperature constant and the other is to keep supply power constant. Temperature control may not be required for a manikin with a constant power supply, but the skin temperatures that result when it is used in non-uniform environments can be unrealistically high or low. This new manikin uses a third method.

The control of this manikin is based on human heat exchange with the thermal environment. The manikin differs from real human beings in that it does not

evaporate moisture from lungs or skin, and this must be taken into account. Heat loss from the human body is expressed as Equation 3-1. Under steady-state conditions, metabolic heat production (M) is almost equal to the total heat loss from a human (Qm). For most indoor work, energy flows due to external work may be assumed to be negligible. Total heat loss (Qm) is divided into that from the skin surface (Qs) and that caused by respiration (Qres). Heat loss from the skin surface (Qs) consists of sensible heat loss (Qt) and latent heat loss (Es), as shown in Equation 3-2. Sensible heat loss (Qt) is in turn divided into radiative (R) and convective (C) heat loss, as shown in Equation 3-3.

$$Qm = M = Qs + Qres \tag{3-1}$$

$$Qs = Qt + Es \tag{3-2}$$

$$Qt = R + C \tag{3-3}$$

Thus, sensible heat loss from the skin surface (Qt) is expressed as Equation 3-4:

$$Qt = Qm - Qres - Es \tag{3-4}$$

According to Fanger (1970) and ASHRAE (1989), heat loss caused by respiration (Qres) and evaporative heat loss from the skin surface (Es) can be expressed as shown below. Here, evaporative heat loss from each body part is unknown; it is not necessary for calculating sensible heat loss from each body part.

$$Qres = 1.7 \cdot 10^{-5} M(5867 - Pa) + 0.0014M(34 - ta) \quad (3\text{-}5)$$

$$Es = 3.05 \cdot 10^{-3}(5733 - 6.99M - Pa) + 0.42(M - 58.15) \quad (3\text{-}6)$$

Here, M is the metabolic rate of a person, and Pa is the partial pressure of water vapor in the air, Since air temperature (ta) is included in the second term of Equation 3-5, it is necessary to measure air temperature to estimate respiration heat loss. To avoid this, air temperature is assumed to be 20℃. This assumption affects only heat loss by respiration, causing a maximum 1.6% error of total heat loss within the range of 10℃ to 30℃ (Tanabe 1994).

According to Fanger's (1970) comfort equation, the mean skin temperature under thermal neutrality may be estimated as Equation 3-7:

$$ts = 35.77 - 0.028Qm \quad (3\text{-}7)$$

Since this thermal manikin is unable to sweat, Q_m cannot be measured directly. For the present purposes, vapor pressure (Pa) is assumed to be 1.5 kPa, which is equivalent to typical indoor conditions at 24℃ and 50% relative humidity (RH). Equation 3-8 may then be derived from Equation 3-1 through Equation 3-7:

$$Qm = 1.96Qt - 21.56 \quad (3\text{-}8)$$

By inserting Equation 3-8 into Equation 3-7, the following equation is obtained:

$$ts = 36.4 - 0.054Qt \tag{3-9}$$

To simulate Equation 3-9, the system controls the skin surface to have a thermal resistance offset of 0.054 m^2℃/w. For example, when the heater temperature is set at 36.4℃ at the first estimation, the heat loss from the skin surface is measured as the electricity consumption of the heating element. However, this relationship between skin surface temperature and heat loss does not satisfy Equation 3-9, so the set point of the skin surface is iteratively changed until it meets Equation 3-9.

In this report, the thermal manikin was controlled to satisfy Equation 3-9. However, this equation may not be applicable under different conditions and different parts of the body. Bischof and Madsen (1991) compared skin temperatures of a thermal manikin like this one with skin temperatures measured on subjects. They showed that the skin temperature of the manikin's feet did not agree with the subjective temperatures, but they found good agreement at other parts of the body. The control equation for individual body parts should probably be adjusted to predict the local skin temperature with more accuracy, but this is going to be very delicate and complex since the thermo-regulation of a real human body involves multiple physiological processes.

3.2 Respiration system (Artificial Lung)

The manikin was equipped with an artificial lung that simulates the human breathing function. The breathing cycle (inhalation, exhalation and pause) and the amount of respiration air as well as temperature and humidity of the exhaled air were controlled. The artificial lungs were adjusted to simulate breathing of an average sedentary person performing light physical work for Asia ethnic according to Huang (1977): breathing frequency of 17 times per minute, volume of 8.5 L/min, breathing cycle of 1.75s inhalation, 1.75s exhalation. The respiration curve approximates the real sinusoidal respiration curve by a hat-top waveform. The air was exhaled from the nose and inhaled through the mouse.

3.2.1 Artificial Lung

The new manikin was connected to an artificial lung, which can create a normal breathing function through the nose and/or the mouth.

The breathing intensity and the breathing frequency can be set at the customer choice.

The inhaled air from the nose and/or the mouth can be transferred to any available analysing equipment for measurement of the air quality exactly in the

breathing zone under realistic conditions. The parameters of artificial lung was list as follow:

Power supply: 110 VAC or 220 VAC, dependent of type.

The output for the air pump can be controlled on the front panel.

The scale is 0 to 100% of 220V ac.

The air flow must be measured with an external equipment.

On the rear panel is placed the output, 0-220VAC max 100 W, for the pump.

Input for control of magnet valves (TTL):

When the valves are disconnected fresh air is supplied to the manikin. When magnets are active, the air from the manikin will be led to analysis.

The 6 air pipe connectors are connected by pressing the pipe to the bottom, and are disconnected by pressing the ring while pulling the pipe.

The pipes between pump and respirator must be short to limit " old air" problems.

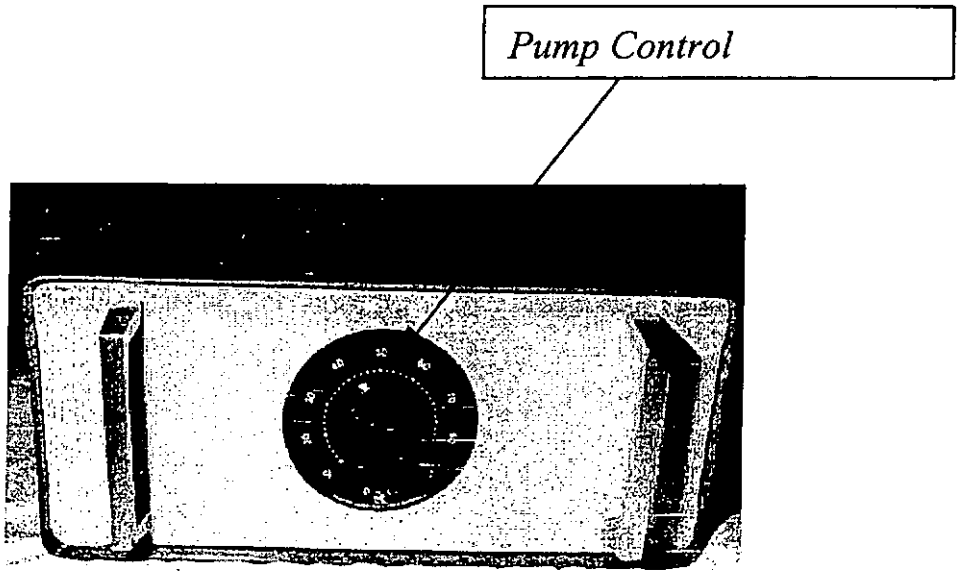

Figure 3.5 The Pump control of Artificial Lung

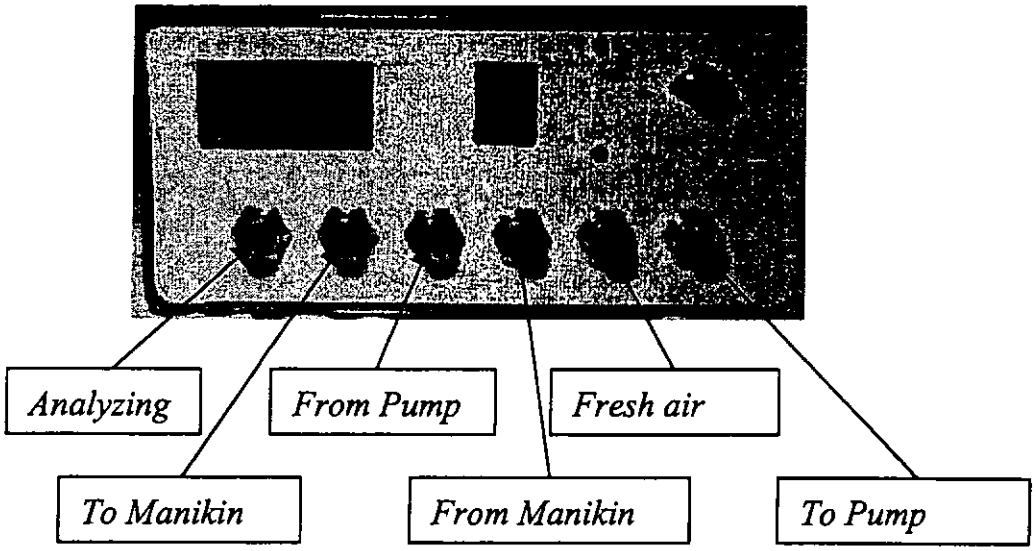

Figure 3.6 The 6 Air pipe connector of Artificial Lung

Breathing intensity can be set from five to twenty litres/minute.

Breathing can be set to any frequency.

The inhaled air can be transferred to any available analysing equipment.

3.2.2 Respiration System

The respiration system with artificial lung was designed in order to simulate realistically the breathing function of a human being and to assess the quality of the inhaled air (Figure 3.8). The air transporting system, which consists of two pumps and two valves, controls the frequency of breathing including duration of exhaled, e.g. the simulated pulmonary ventilation. The respiration curve approximates the real sinusoidal respiration curve by a hat-top waveform. The

respiration frequency is about 3.5 s, with a time-mean airflow rate about 0.14 l/s (8.5 l/min) as shown on Figure 3.7.

The measurement interval of the CO_2 meters is 30 s, which is longer than the respiration cycle. Therefore, the monitored CO_2 concentration can be considered as the time-mean value of the inhaled air, as shown in Figure below.

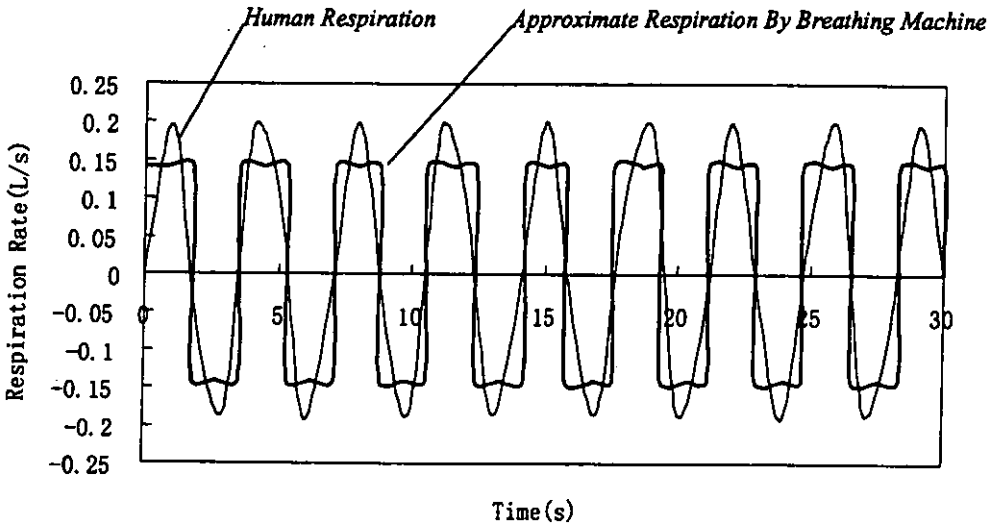

Figure 3.7 Human Respiration and Approximate Respiration by the Breathing Machine

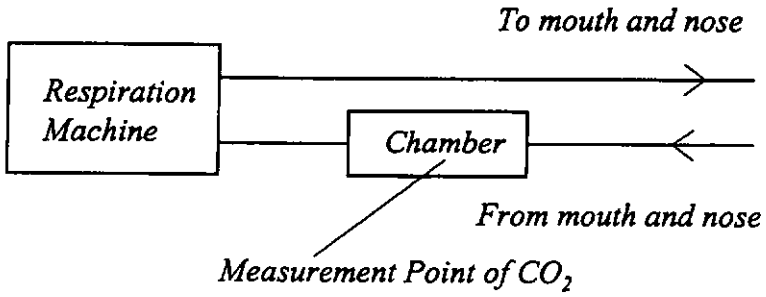

Figure 3.8 Configuration of breathing system of the thermal manikin

A TSI facility real time CO_2 monitor Q-Trak was used to measure the CO_2 concentration of inhaled air. The probe of Q-Trak was a cylinder with 0.183m in length. The maximum value it could measured was 6000 ppm, the accuracy is 1%.

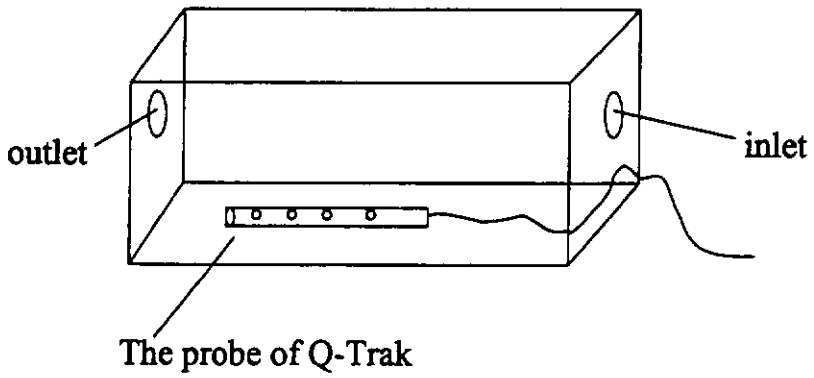

Figure 3.9 The chamber setting for measure the CO_2 concentration of inhaled air

A chamber was built in the inhalation section to deposit the probe of Q-Trak and measure the CO2 concentration of inhaled air. The chamber was 0.25*0.25*0.4 m^3. Some pipes connect the chamber with nose/mouth and artificial lung just as trachea of human being.

3.3 Personalized air system

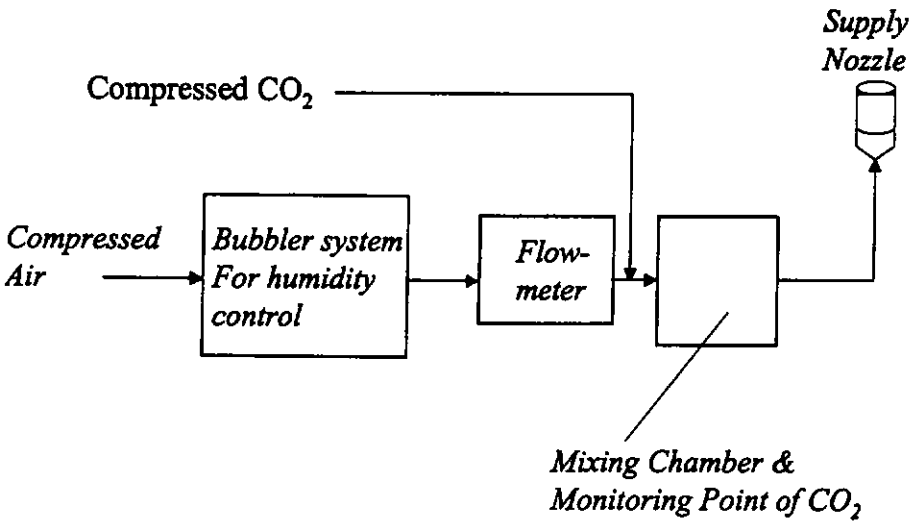

Figure 3.10 Configuration of supply air system

The compressed air was used as the supplied air in personalized ventilation system. A bubbler system was added on the ventilation system, which makes the humidity of supplied air could be controlled. A flow meter was used to measure the personalized ventilation rate. A chamber was used in the system to mixture the compressed air and compressed CO_2. A flexibility tube connected the chamber and air terminal device (supply nozzle). The air terminal nozzle is located at the chin position. Of this air, only 0.1 l/s or 1% is inhaled. For the "personalized air", the fresh air is directed to the breathing zone of each individual. In this series of experiments, the supplied airflow rates were set

raging from 0.1 l/s to 3 l/s, and the supply air temperature and humidity is close to room air temperature.

The tracer gas CO_2 was used in the experiments. The concentration of CO_2 in the compressed air is 334ppm. The concentration of ambient air fluctuated between 500ppm to 700ppm. A pure compressed CO_2 was used to mixture with compressed air in chamber that make the CO_2 concentration far higher than that of ambient air (about 2000ppm~5000ppm depending on supply airflow rates tested). The CO_2 concentration of supplied air and ambient air were directly measured using the Q-Trak real time CO_2 monitors.

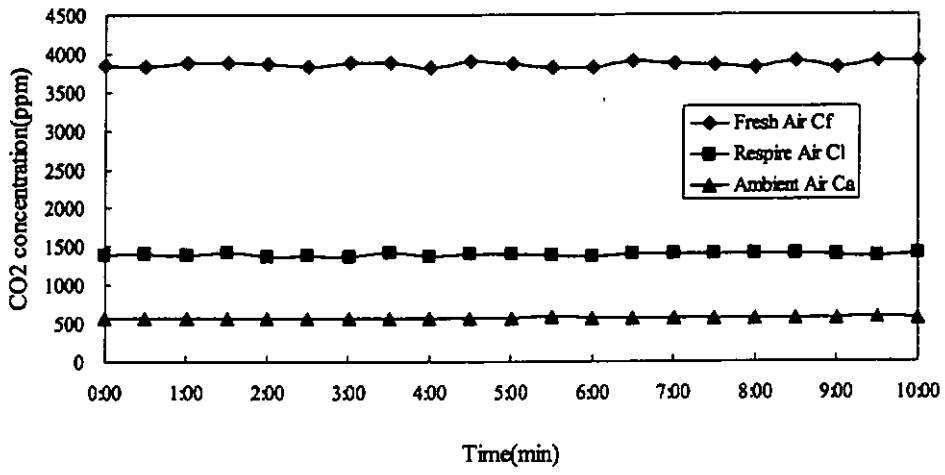

Figure 3.11 CO_2 concentrations in fresh air, inhaled air, and ambient air measured at fresh airflow rate of 0.5 l/s

3.4 Experimental conditions

An actual office was used as the test chamber. The chamber was 9×3×3 m^3, with a partition wall placed in the middle of the room. A convention air-conditioning system has been in operation to provide general ventilation and to maintain temperature and relative humidity of the air inside the chamber. The velocity generated by the ventilation system in the chamber is lower than 0.05 m/s. The climate chamber temperature was 21℃ and humidity was 60%.

3.5 Air terminal device

In Melikov's study, the PEE reached the high point at around 7 L/s, it was not advanced as the supply ventilation flow rate further increased. For this study, the supplied air terminal device (SATD) was schematically located at the chin position so much higher pollutant exposure reduction index η_{PER} could be expected and maximal airflow rate could be reduced. The angle and distance of SATD is fixed in this series of experiments.

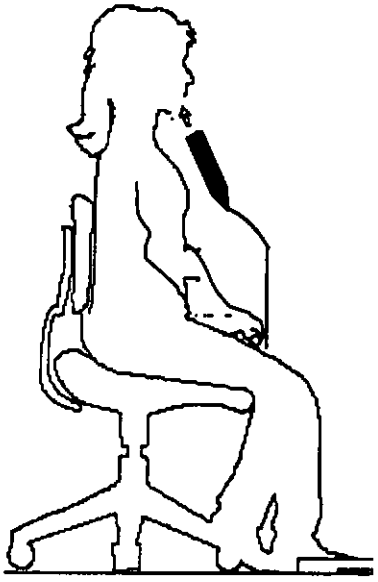

Figure 3.12 the air terminal device was locate at the chin position

Four rectangular air terminal devices LSRN, MSRN, SSRN, FSRN and four circular air terminal devices LCN, MCN, SCN, SSCN were developed and studied. The LSRN was 0.15m in length and 0.07m in width. The MSRN was 0.1m in length and 0.05m in width. The SSRN was 0.1m in length and 0.03m in width. And the FSRN was 0.12m in length and 0.03m in width. The LCN with the diameter 0.12m has the same effective area as LSRN. The MCN's diameter was 0.1m. The SCN with diameter 0.08m has the same effective area as MSRN. The SSCN's diameter was 0.06m.

In the supplied air system, the diameter of flexibility tube which connected the chamber and air terminal device was 0.3m. To ascertain that a uniform velocity profile is obtained at the outlet of the nozzle, restricted stream analysis was introduced to adjust the geometry of the ATD.

For the circular nozzle LCN, when the supply airflow rate was 3 l/s, the air velocity of airflow in the flexible tube was 4.2m/s. Thus, the maximal circumfluence air velocity $V_{h,p}$

$$v_{h,p} = 0.69 \times v_0 \times d_0 \Big/ \sqrt{F_n} = 0.69 \times 4.2 \times 0.03 \Big/ \sqrt{\pi \times (0.12)^2 / 4} = 0.8 m/s \quad (3\text{-}10)$$

Where F_n: the cross section area of circular nozzle

v_0: the stream velocity

d_0: the diameter or equivalent diameter of flexible tube

The dimensionless distance in the second section is

$$X = ax \Big/ \sqrt{F_n} = 0.076 \times 0.2 \Big/ \sqrt{\pi \times (0.12)^2 / 4} = 0.14m \quad (3\text{-}11)$$

For gradually expanding section: $L = \dfrac{(d - d_0)/2}{\sin(10\pi/180)} = 0.3m$

Then the total length of the air terminal device LCN was determined to be 0.14+0.3 = 0.44m

For the rectangular-cross-sectional series, similar analysis were understake to determine their geometries.

3.6 experimental measuring procedures

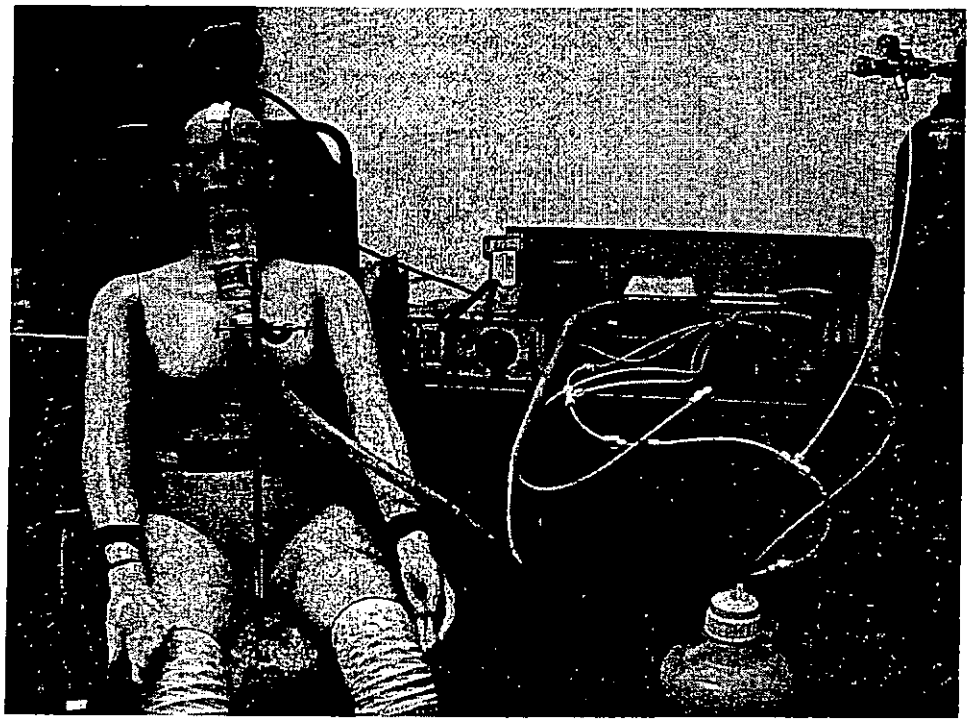

Figure 3.13 the personalized air system

A tracer gas, CO_2, was mixed into the personalized air. The concentration of the tracer gas (CO_2) was measured in the test chamber, in the air supplied by the personalized ventilation system and in the air inhaled by the breathing thermal manikin. A gas monitor Q-Trak based on the photo acoustic infrared detection method of measurement measured the concentration of CO_2 continuously. The concentration measured under steady-state conditions during the last 10 min of each experiment was averaged and analyzed. Seven series experiments with air flow rate 0.1 l/s, 0.4 l/s, 0.8 l/s, 1.5 l/s, 2 l/s, 2.5 l/s, 3 l/s, 4 l/s for each ASTD was developed. The supply air temperature was 21°C, the same as the climate

chamber. The humidity of the supply air was maintained around at 36% in this series of tests.

CHAPTER IV: EXPERIMENT RESULTS AND DISCUSSION

In this series of experiments, the artificial lungs were adjusted to simulate breathing of an average sedentary person performing light physical work: breathing frequency was set up to 17 times per minute or 3.5s per breathing cycle volume 8.5 l/min (0.14 l/s). The respiration curve approximates the real sinusoidal respiration curve by a hat-top waveform.

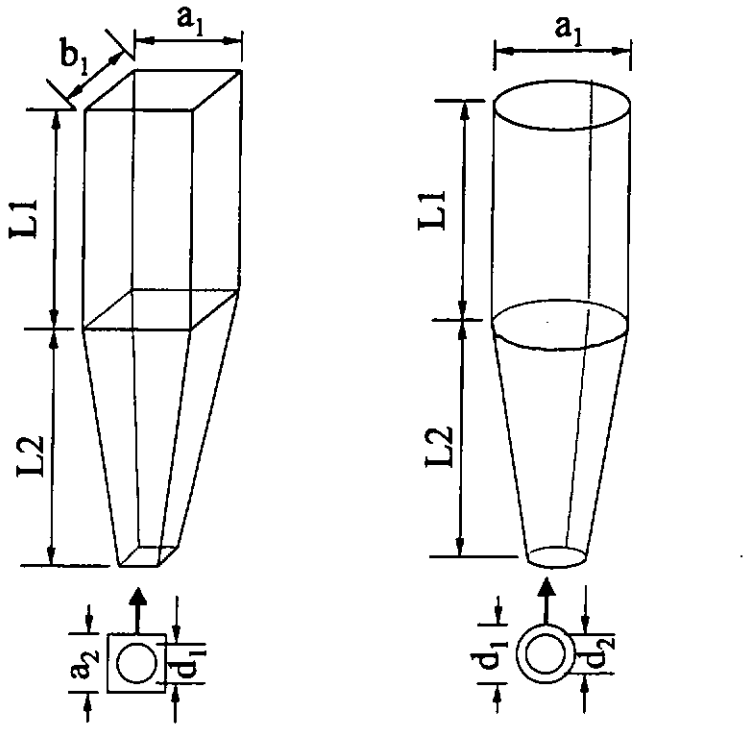

Figure 4.1. Air Terminal Devices tested

Four rectangle air terminal devices (The large air terminal device – LSRN, the middle one – MSRN, the standard one – SSRN and the flat rectangular one – FSRN) and four

circular air terminal devices (circular air terminal device with 120mm diameter – LCN, with 100mm diameter – BCN, with 80mm diameter – SCN and with 60mm diameter – SSCN) were developed and studied. The air terminal devices are schematically shown in Figure 4.1, and the geometry details are given in Table 4.1.

The left-hand of figure was the schematic figure of rectangular air terminal device and the right-hand was the circular air terminal device. The air terminal device was connected to the personalized air supply system with flexible tube as shown in Figure 3.10.

Table 4.1 the dimension of air terminal devices

	L1(mm)	L2(mm)	a1(mm)	b1(mm)	a2(mm)	d1(mm)	d2(mm)
LSRN	230	270	150	70	30	28	
MSRN	150	200	100	50	30	28	
SSRN	150	200	100	30	30	28	
FSRN	150	200	120	30	30	28	
LCN	230	270	120			30	28
MCN	150	200	100			30	28
SCN	150	200	80			30	28
SSCN	150	200	60			30	28

In the series of testing using a heating thermal manikin, the personal supply airflow rate V_L was set from 0.1 l/s to 3 l/s. The personal supply air temperature was set at 20 ℃ that is close to room temperature. For the heated thermal manikin, the mean skin temperature under occupant's thermal comfort (Tanabe et al 1994) was defined as the temperature of a uniform enclosure in which a thermal manikin would lose heat to the environment at the same rate as it would in the actual environment. It was calculated by the following expression that mentioned in Chapter III:

$$ts = 36.4 - K \cdot Qt \tag{4-1}$$

where 36.4 is the deep body temperature, ℃

ts is the skin temperature

Qt is measured sensible heat loss, W/m^2

K is thermal resistance offset of the skin temperature control system of the thermal manikin equal to 0.054 m^2℃/w

In this series of experiment, the temperature of thermal manikin was around 32℃, depending on the different body part. This control was realized with the computerised control of the 16 built-in independent heaters and skin surface temperature sensors.

Table 4.2 The 20 body parts surface skin temperature

L.Foot	R. Foot	L. low leg	R. low leg	L.Front thigh	L.Back thigh
30. 4℃	30. 6℃	31. 4℃	31. 4℃	31. 7℃	33. 2℃
R.Front theigh	R.Back thigh	Pelvis	Backside	Face	Crown
31. 7℃	33. 2℃	31. 9℃	32. 6℃	31. 6℃	32. 7℃
L.hand	R. Hand	L.forearm	R.forearm	L.upper arm	R.upper arm
30. 8℃	31. 1℃	31. 5℃	31. 6℃	31. 3℃	31. 6℃
Chest	Back				All
32. 2℃	32. 6℃				31. 9℃

As mentioned in Chapter II, the pollutant exposure reduction index η_{PER} was calculated by the following expression:

$$\eta_{PER} = \frac{(C_{a,P} - C_{L,P)}}{C_{a,P}} = 1 - \frac{C_{L,P}}{C_{a,P}} \tag{4-2}$$

Where, $C_{a,P}$ is pollutant concentration in ambient air, ppm

$C_{L,P}$ is pollutant concentration in inhaled air, ppm

Numerically, η_{PER} is equal to the fraction of fresh air in inhaled air, which is in turn defined as ventilation coefficient η_f and can be calculated from the measured tracer gas CO_2 concentrations:

$$\eta_f = \frac{V_{F,L}}{V_L} = \frac{C_L - C_a}{C_F - C_a} \tag{4-3}$$

Where, C_F is CO_2 concentration of the fresh air supply, ppm

C_a is CO_2 concentration of ambient room air, ppm

C_L is CO_2 concentration of inhaled air, ppm

In our tracer gas measurements, the CO_2 concentration of the supply air was set about 2000ppm ~ 5000ppm depending on supply airflow rates, which was much above the CO_2 concentration of the ambient room air, which was about 500ppm ~ 700ppm. All the CO_2 concentration of supply air, ambient air and inhaled air were directly measured by real time CO_2 monitors Q-Trak.

The purpose of personalized ventilation is to achieve the highest possible quality of the air inhaled by occupants by providing clean air at the breathing zone. Thus the quality of the inhaled air when personalized ventilation is applied has to be better than with a total-volume ventilation system (mixing and displacement). Ideally, the inhaled

air should consist of 100% personalized air, in other words, pollutant exposure reduction index η_{PER} should be equal to 1.

4.1 The effect of thermal plume around Human body

As we know, in a calm, comfortable environment, upward free convection movement exists around the human body due to the temperature difference between the room air the surface of the clothing and of the skin of bare body parts. The free convection flow becomes weak when the temperature difference is small. The airflow is slow and laminar with a thin boundary layer at the lower body parts, and fast and turbulent with a thick boundary layer at the height of the head.

The free convection movement will change the skin temperature due to convection heat transfer and will thus affect man's thermal sensation. The free convection flow transports air, which might be contaminated from the lower part of the space, upward to the breathing zone.

One type of air terminal device (circular nozzles with 120mm diameter) was tested with a heating thermal manikin and a non-heating thermal manikin, respectively. The supply airflow rate V_L was set from 0.1 l/s to 2 l/s. The supply air temperature was set at 20℃ that is close to room temperature.

Table 4.3 The C_f, C_a, C_L and η_f of this series of tests

flowrate	Heating Thermal Manikin				Non-heating Thermal Manikin			
l/s	C_f(ppm)	C_L(ppm)	C_a(ppm)	η_f	C_f(ppm)	C_L(ppm)	C_a(ppm)	η_f
0.1	4837	670	580	0.02	4672	730	560	0.04
0.5	3243	1112	602	0.19	3028	1209	596	0.25
1.0	4942	1799	614	0.27	4865	1976	612	0.34
1.5	2840	1363	633	0.33	2954	1562	620	0.40
2.0	2623	1429	650	0.39	2734	1531	631	0.43

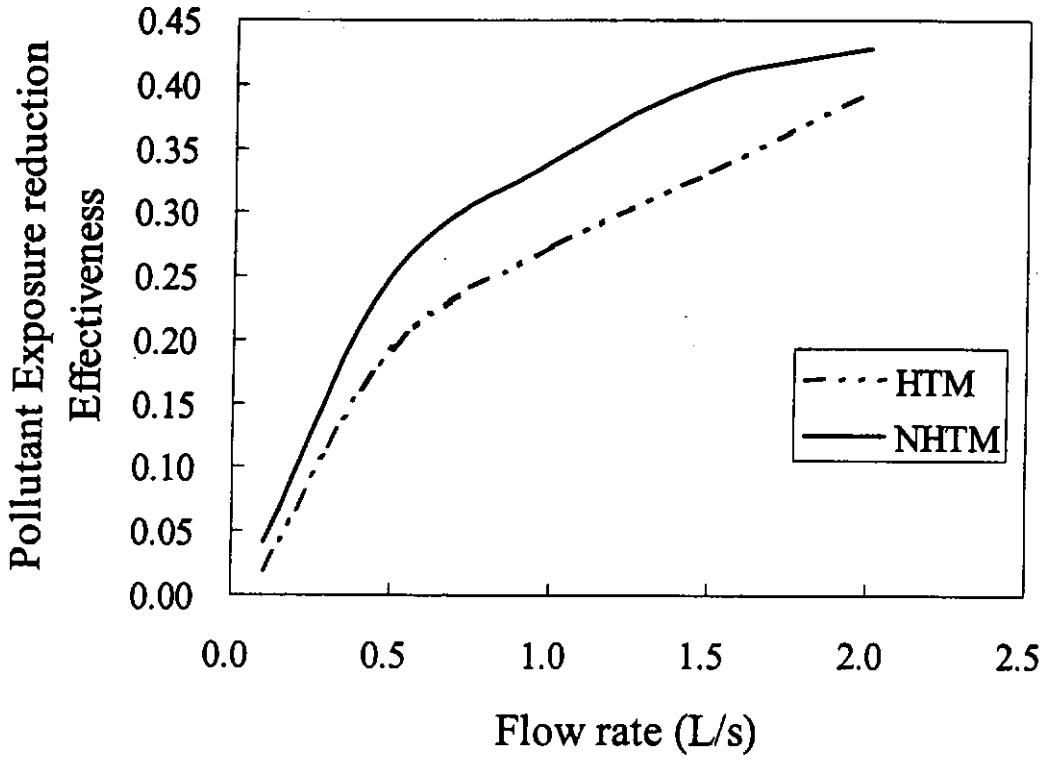

Figure 4.2 Pollutant exposure reduction effectiveness as a function of the airflow rate from air terminal device: isothermal condition: room air 20℃, personalized air temperature 20℃. Non-isothermal condition: room air 22℃, personalized air temperature 20℃, the skin temperature of thermal manikin 31℃.

As shown on Figure 4.2, the Pollutant Exposure reduction Effectiveness was affected obviously by the free convection flow rate around the human body due to the temperature difference between the room air and the thermal manikin. The interaction between the airflow from the personalized ventilation, the free convection flow

around the body and the airflow of exhalation is of primary importance for occupants' thermal comfort and pollutant exposure reduction effectiveness.

As shown on Figure 4.2, the exits of free convection flow rate around the human body reduce the pollutant exposure reduction effectiveness. The pollutant exposure reduction effectiveness η_{PER} of the air terminal device in heating thermal manikin system ranges from 0.02 to 0.39 within the supplied airflow range from 0.1 to 2 l/s and in the non-heating thermal manikin system, the range is from 0.04 to 0.43. The slope of the curve air terminal device in non-heating thermal manikin system in the range of 1.0 to 2.0 l/s appears small than that of in heating thermal manikin system, indicating that the free convection flow rate around the human body will have limited effects on pollutant exposure reduction effectiveness at higher flow rate. These effects can be better seen in Table 4.4. It appears that, when the personal air supply flow rate is low, the impact, as indicated by the effective factor in the last column, is more obvious. As the personal air supply rate becomes higher, the impact of the thermal plume becomes weak.

Table 4.4 The effects of free convection on pollutant exposure reduction effectiveness under different personalized airflow rate

flowrate	Heating Thermal Manikin	Non-heating Thermal Manikin	Effective factor
l/s	η_{PER}	η_{PER}	
0.1	0.02	0.04	95.55%
0.5	0.19	0.25	30.53%
1.0	0.27	0.34	24.18%
1.5	0.33	0.40	22.02%
2.0	0.39	0.43	8.39%

4.2 The effect of airflow rate

The pollutant exposure reduction effectiveness of the studied air terminal devices (ATDs – LSRN, MSRN, SSRN, FSRN, LCN, MCN, SCN, SSCN) is compared in Table 4.5 and Figure 4.3. The pollutant exposure reduction effectiveness as a function of the flow rate is shown in the figures. Common characteristics for the ATDs studied can be identified. The results showed that an increase in the flow rate from zero has no immediate effect on the pollutant exposure reduction effectiveness. Only when a certain initial flow rate is reached does the pollutant exposure reduction effectiveness for most of the ATDs studied start to increase rapidly with the flow rate. It is also clear from the results shown in the figures that the increase in the pollutant exposure reduction effectiveness becomes marginal at a certain flow rate until it reaches a steady-state maximum value. The maximum pollutant exposure reduction effectiveness was found to be different for the ATDs investigated.

Table 4.5 The C_f, C_a, C_L and η_f of this series of tests

Flowrate	L/s	0.1	0.4	0.8	1.5	2	2.5	3
	C_f(ppm)	4725	1913	3549	2763	2317	1983	1719
	C_L(ppm)	783	902	1329	1444	1409	1370	1260
LSRN	C_a(ppm)	613	610	605	600	594	580	560
	η_f	0.04	0.22	0.25	0.39	0.47	0.56	0.60
	C_f(ppm)	4032	2466	4586	3101	2570	2195	1808
MSRN	C_L(ppm)	1125	1335	2356	1871	1787	1665	1429
	C_a(ppm)	620	618	612	607	602	591	580
	η_f	0.15	0.39	0.44	0.51	0.60	0.67	0.69
	C_f(ppm)	4531	3542	2583	3403	2487	1930	1690
SSRN	C_L(ppm)	1097	1195	1088	1640	1427	1331	1242
	C_a(ppm)	680	680	662	653	640	633	621
	η_f	0.11	0.18	0.22	0.36	0.43	0.54	0.58
	C_f(ppm)	4178	2647	2516	3269	2792	2039	1818
FSRN	C_L(ppm)	1778	1594	1562	1828	1600	1265	1191
	C_a(ppm)	1302	1100	930	790	650	480	480
	η_f	0.17	0.32	0.40	0.42	0.44	0.50	0.53
	C_f(ppm)	4837	3116	4672	2840	2623	2213	1897
LCN	C_L(ppm)	670	1004	1799	1463	1429	1432	1307
	C_a(ppm)	580	600	614	650	650	657	660
	η_f	0.02	0.16	0.29	0.37	0.39	0.50	0.52
	C_f(ppm)	4960	3236	2275	4012	2727	2300	1887
MCN	C_L(ppm)	1282	1399	1524	2780	2039	1777	1505
	C_a(ppm)	620	612	605	600	588	576	560
	η_f	0.15	0.30	0.55	0.64	0.68	0.70	0.71
	C_f(ppm)	5486	4300	3136	1663	3210	2642	2411
SCN	C_L(ppm)	1382	2016	1926	1231	2349	2139	2019
	C_a(ppm)	540	532	520	498	482	470	464
	η_f	0.17	0.39	0.54	0.63	0.68	0.77	0.80
	C_f(ppm)	3218	1978	1087	3711	2122	2800	1980
SSCN	C_L(ppm)	1002	1036	862	2662	1644	2162	1620
	C_a(ppm)	526	524	511	502	480	472	460
	η_f	0.18	0.35	0.61	0.67	0.71	0.73	0.76

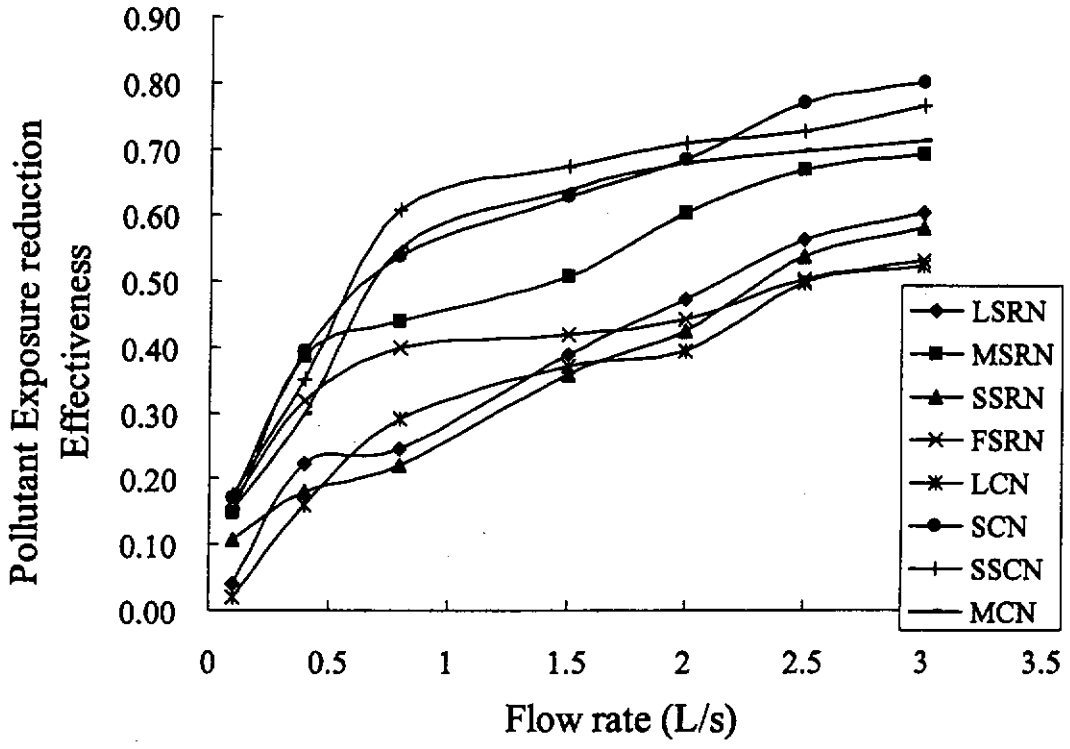

Figure 4.3 Pollutant exposure reduction effectiveness as a function of the airflow rate from air terminal device: Non-isothermal conditions: room air temperature 22℃, personalized air temperature 20℃, the skin temperature of thermal manikin 31℃. LSRN (the largest rectangular nozzle), MSRN(the middle size rectangular nozzle), SSRN (the small size rectangular nozzle), FSRN (the flat rectangular nozzle), LCN(the largest circular nozzle), MCN(the middle size circular nozzle), SCN(the small size circular nozzle), SSRN (the smallest circular nozzle)

The results of this investigation showed that for the flow rates studied, the ATDs were not able to provide 100% of personalized air in the occupant's inhalation. This also get from the preliminary investigation (Melikov 2001), it showed that for the flow rates studied (up to 23 L/s) the air terminal devices were not able to provide 100% of personalized air in the occupant's inhalation. Even if in our investigation, the supply nozzles were located at chin position, the pollutant exposure reduction effectiveness could not got 1, or in other words the air terminal devices were not able to provide 100% pure fresh air in the occupant's inhalation. The performance of the ATDs changed as the flow rate increased. The results in Figure 4.3 show that a maximum

pollutant exposure reduction effectiveness of 0.8 was achieved by the SCN at a minimum airflow rate of 3 L/s. The maximum pollutant exposure reduction effectiveness achieved by the ATDs appeared not to increase with the further increase of the area of cross section of ATDS, but this needs to be verified with real experiments at higher airflow rate conditions.

Table 4.6 the η_f of SCN (small circular ATD) as the function of airflow rate

Flowrate	L/s	0. 1	0. 4	0. 8	1. 5	2	2. 5	3
SCN	η_f	0. 17	0. 39	0. 54	0. 63	0. 68	0. 77	0. 80

For the air terminal device SCN, the η_{PER} ranges from 0.17 to 0.80 within the supplied airflow range from 0.1 to 3 l/s. It appears that the pollutant exposure reduction effectiveness increase rapidly from 0.17 to 0.39 as the air flow rate from 0.1 to 0.4 l/s and η_{PER} curves are becoming flat as airflow increases further from 2.5 l/s. This may indicate that increasing supplied airflow with a given supply air terminal device will have limited effects on increasing the efficiency or we could see it reaches a steady-state maximum value. Figure 4.4 shown the $\Delta_{\eta PER}/\Delta_{\text{flow rate}}$ as the airflow rate from 0.1 to 3 l/s.

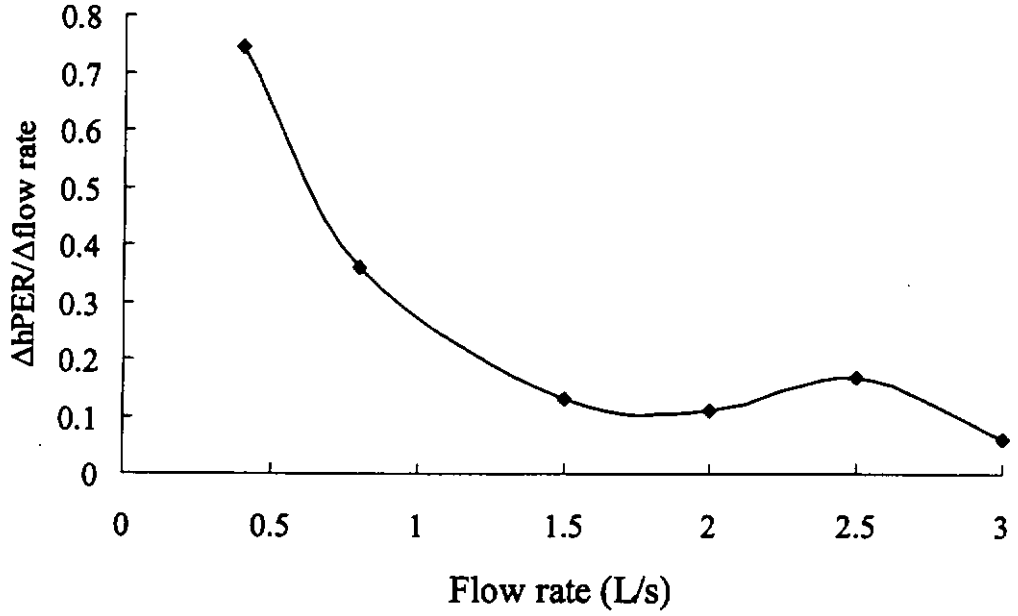

Figure 4.4 the $\Delta_{\eta PER}/\Delta_{flow\ rate}$ as a function of the airflow from air terminal device SCN

Another index called fresh air utilization efficiency η_u is defined that expresses the ratio of actual fresh air in the inhaled air to the supplied fresh air, and can be calculated as:

$$\eta_u = \eta_f * V_L / V_f \qquad (4\text{-}4)$$

Table 4.7 The η_u of the series of tests

Flowrate(L/s)	0. 1	0. 4	0. 8	1. 5	2	2. 5	3
LSRN	0. 05788	0. 07843	0. 04304	0. 03642	0. 03311	0. 03153	0. 02819
MSRN	0. 20721	0. 1358	0. 0768	0. 0473	0. 04215	0. 0375	0. 03226
SSRN	0. 1516	0. 06298	0. 03881	0. 0335	0. 02983	0. 03014	0. 02711
FSRN	0. 23171	0. 11176	0. 06974	0. 03908	0. 03105	0. 0282	0. 0248
LCN	0. 0296	0. 0562	0. 0511	0. 03465	0. 02764	0. 02789	0. 02441
MCN	0. 21355	0. 10496	0. 0963	0. 05963	0. 04749	0. 03901	0. 03323
SCN	0. 23832	0. 13785	0. 09405	0. 05872	0. 04791	0. 04303	0. 03726
SSCN	0. 24755	0. 12327	0. 10661	0. 06282	0. 04963	0. 04065	0. 03561

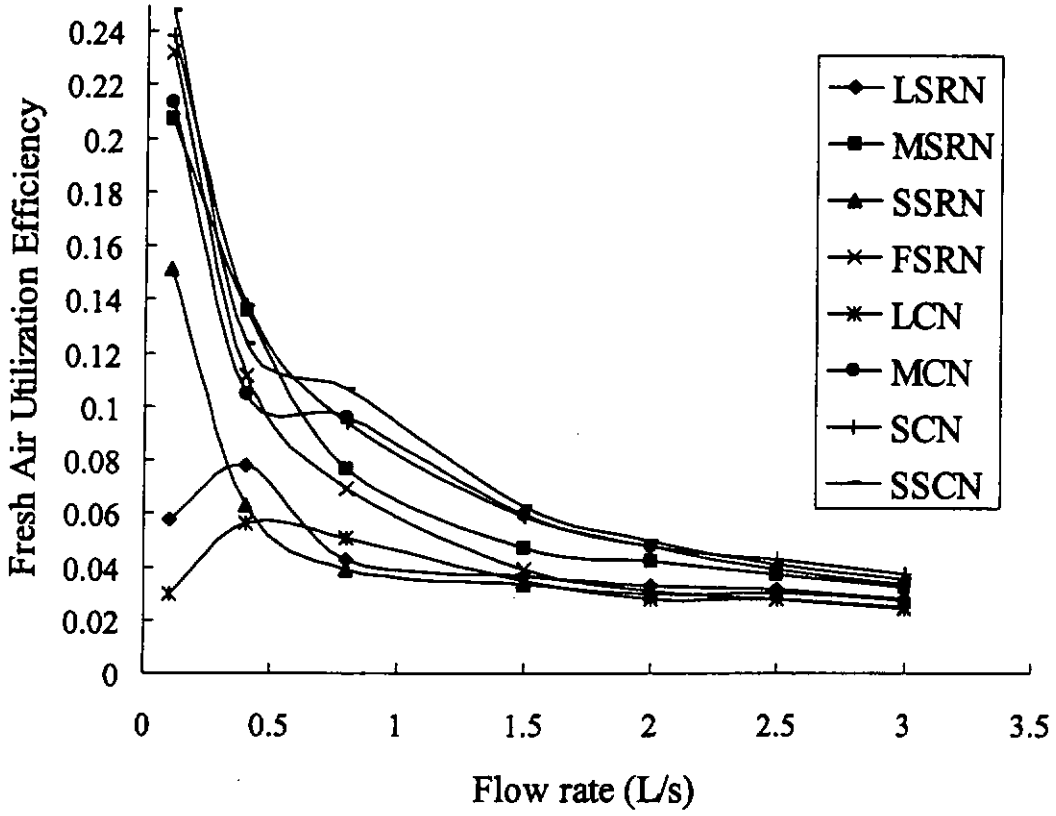

Figure 4.5 fresh air utilization efficiency as a function of the airflow rate from air terminal device: Non-isothermal conditions: room air temperature 22℃, personalized air temperature 20℃, the skin temperature of thermal manikin 31℃. LSRN (the largest rectangular nozzle), MSRN (the middle size rectangular nozzle), SSRN (the small size rectangular nozzle), FSRN (the flat rectangular nozzle), LCN(the largest circular nozzle), MCN(the middle size circular nozzle), SCN(the small size circular nozzle), SSRN (the smallest circular nozzle)

As shown in Figure 4.5, the utilization efficiency η_u decreases as the supplied airflow rate increases from 0.1 to 3 l/s. The maximal of η_u is about 0.25 or 25% at lower flow rates, and becomes lower 0.02 or 2% as the supply air rate is increased to in 3 l/s. For the air terminal device SCN is 0.037 or 3.7%. This is still much higher than 1% - maximum that can be achieved in conventional ventilation systems.

Combined with curve of pollutant exposure reduction effectiveness η_{PER}, the increase of airflow rate will increase the pollutant exposure reduction effectiveness η_{PER} but

decrease the utilization efficiency η_u. The pollutant exposure reduction effectiveness represents the inhaled air quality and probably also the inhaled air thermal sensation when cool air is supplied; whereas the utilization efficiency represent the supply air utilization efficiency. Therefore the overall results mean that more airflow rate will produce better inhaled air quality and inhaled air thermal sensation but will reduce the supply air utilization efficiency. Both the figure of pollutant exposure reduction effectiveness and the figure of utilization efficiency shown that the slope of curve become flat as the airflow rates increase further at certain value. Thus, we may take airflow rate at the which the two curves appear to be flat as the optimum air supply flow rate so that the best inhaled air quality is nearly achieved while the supply air utilization efficiency can be still much higher than that of the conventional well-mixed ventilation systems, which is typically around 0.01.

The present standards and guidelines recommend ventilation rates from 4 to 10 L/s peroccupant in offices without smoking and up to 30 L/s per occupant when some smoking is allowed (ASHRAE Standard 62 1989, CR 1752 1998). ATD with large outlets, providing laminar airflow with a low velocity which will not cause draught discomfort for the occupants, has been previously suggested (Melikov 1999) as one of the design recommendations for personalized ventilation systems. Such ATD will make it possible to provide the high airflow rate of 30 L/s per occupant, as recommended in the guidelines (CR 1752 1998), without local thermal discomfort. In practice, however, most often 10 L/s per occupant may be required. The studies of Melikov (2001) indicate that under these conditions it will be rather difficult to use large ATD. Better results will be achieved by relatively small ATD, compromising for the inhaled air quality. In these studies, the air terminal devices were directly located

at the chin position of thermal manikin, the supplied air was directly fused into breathing zone. By observing the variation trend of the pollutant reduction effectiveness vs the air supply flow rate in Figure 4.3, it can be seen that, the pollutant reduction effectiveness reaches 0.8 at 3 L/s, which is already a good achievement. Considering that thermal comfort may be adversely affected due to draught at higher air speed, 3 L/s may be the good enough for the supplied airflow rate. But this needs to be verified with further investigations.

Actually, for different area and geometry of air terminal devices, the effects of air flow rate on pollutant exposure reduction effectiveness are different. These will be discussed at the other sections.

4.3 The effect of air terminal devices area

With the same supply airflow rate, the different area of air terminal devices will produce different supply air velocity and different supply air area. The microclimate of breathing zone will be affected, and also the pollutant exposure reduction effectiveness.

4.3.1 the rectangular air terminal devices

Table 4.8 The C_f, C_a, C_L and η_f of three series rectangular nozzles with different area (The large size nozzle, the middle size nozzle, the small nozzle and the flat nozzle)

Flowrate	0.1	0.4	0.8	1.5	2	2.5	3
	4725	1913	3549	2763	2317	1983	1719
LSRN	783	902	1329	1444	1409	1370	1260
	613	610	605	600	594	580	560
	0.04	0.22	0.25	0.39	0.47	0.56	0.60
	4032	2466	4586	3101	2570	2195	1808
MSRN	1125	1335	2356	1871	1787	1665	1429
	620	618	612	607	602	591	580
	0.15	0.39	0.44	0.51	0.60	0.67	0.69
	4531	3542	2583	3403	2487	1930	1690
SSRN	1097	1195	1088	1640	1427	1331	1242
	680	680	662	653	640	633	621
	0.11	0.18	0.22	0.36	0.43	0.54	0.58
	4178	2647	2516	3269	2792	2039	1818
FSRN	1778	1594	1562	1828	1600	1265	1191
	1302	1100	930	790	650	480	480
	0.17	0.32	0.40	0.42	0.44	0.50	0.53139

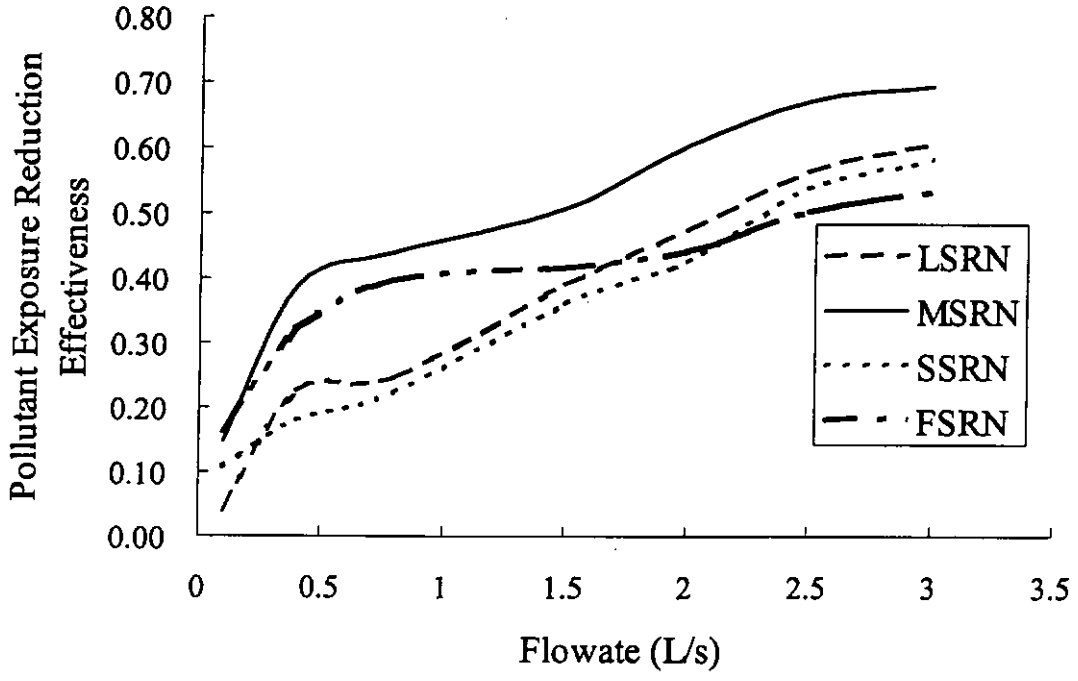

Figure 4.6 Pollutant exposure reduction effectiveness as a function of the airflow rate from rectanguiar air terminal device: Non-isothermal conditions: room air temperature 22℃, personalized air temperature 20℃, the skin temperature of thermal manikin 31℃. LSRN (the largest rectangular nozzle), MSRN (the middle size rectangular nozzle), SSRN (the small rectangular nozzle), FSRN (the flat rectangular nozzle)

The cross section of air terminal device LSRN, MSRN, SSRN and FSRN are rectangular. The LSRN has the largest cross-sectional area in the rectangular ATDs been investigated. MSRN has same proportion between the long sides and the short sides with LSRN but the area of cross section is different. The cross section area of LSRN is 1.5 times large than MSRN. The length of long side of SSRN was the same as that of MSRN. But the length of short side was shorter than that of MSRN. The FSRN has the same effective area with air terminal device MSRN but different proportion between the long side and the short side. The results in figure show that the slope of the LSRN curve becomes flat at about 3 L/s, and the slope of the MSRN becomes flat at about 2.5 L/s, the slope of the SSRN curve becomes flat at about 3 L/s, and the slope of the FSRN becomes flat at about 3 L/s. The maximum pollutant exposure reduction effectiveness was reached by LSRN was 0.6, and for the MSRN, was 0.69. The maximum pollutant exposure reduction effectiveness was reached by SSRN was 0.58, and for the LCN, was 0.53.

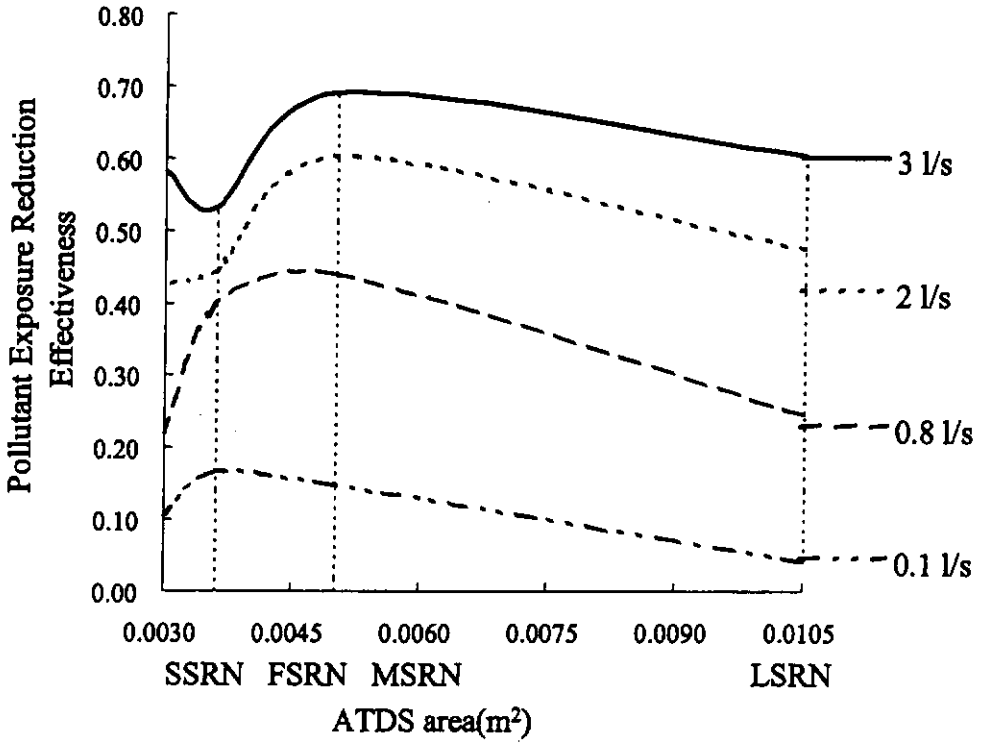

Figure 4.7 Pollutant exposure reduction effectiveness as a function of the area of rectangular air terminal device: Non-isothermal conditions: room air temperature 22 ℃, personalized air temperature 20℃, the skin temperature of thermal manikin 31℃. LSRN (the largest rectangular nozzle), MSRN (the middle size rectangular nozzle), SSRN (the small rectangular nozzle), FSRN (the flat rectangular nozzle)

As shown on Figure 4.7, at a fixed flow rate, the pollutant exposure reduction effectiveness varies with the cross-sectional area of ATDs. The increasing of cross-area helps to increase the pollutant exposure reduction effectiveness in the smaller area size range. However, it is not to say that pollutant exposure reduction effectiveness will increase further as an ATD's cross-area exceeds a certain value. The peak value reached at a certain middle area with certain airflow rate. After this area, the pollutant exposure reduction effectiveness will decrease with the further increasing of ATDs' cross-area. In this series of experiments, for supply airflow rate

of 3 l/s, the maximum pollutant exposure reduction effectiveness reached 0.6 with MSRN.

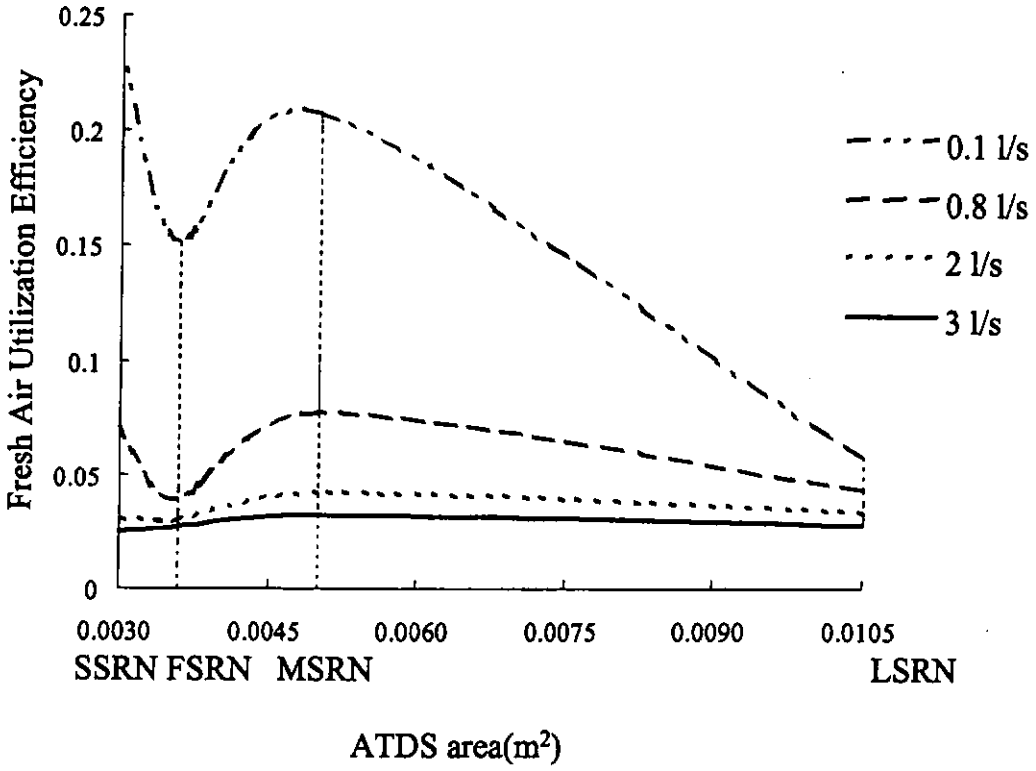

Figure 4.8 Fresh air utilization efficiency as a function of the ATDs area from rectangular air terminal device: Non-isothermal conditions: room air temperature 22 ℃, personalized air temperature 20℃, the skin temperature of thermal manikin 31℃. LSRN (the largest rectangular nozzle), MSRN (the middle size rectangular nozzle), SSRN (the small size rectangular nozzle), FSRN (the flat rectangular nozzle)

As shown on Figure 4.8, at the same airflow rate, the fresh air utilization efficiency varies with the cross-sectional area of ATDs. Opposite to the pollutant exposure reduction effectiveness, the increasing of cross-area will decrease the fresh air utilization efficiency. The obvious difference of fresh air utilization in different type of ATDs exists when the airflow rate is 0.1 l/s. At higher airflow rate, the difference between different ATDs becomes less obvious. As the airflow rate equal to 3.0 l/s, the

slope almost become flat, or in other words, the change of ATDs' cross-area will not affect the fresh air utilization efficiency.

4.3.2 The circular air terminal devices

Similar conclusion also could be dran in circular air terminal devices.

Table 4.9 The C_f, C_a, C_L and η_f of three series circular nozzles (The large size circular nozzle, the middle size circular nozzle, the small size circular nozzle and the smallest circular nozzle)

Flowrate	0. 1	0. 4	0. 8	1. 5	2	2. 5	3
	4837	3116	4672	2840	2623	2213	1897
LCN	670	1004	1799	1463	1429	1432	1307
	580	600	614	650	650	657	660
	0. 02	0. 16	0. 29	0. 37	0. 39	0. 50	0. 52
	4960	3236	2275	4012	2727	2300	1887
MCN	1282	1399	1524	2780	2039	1777	1505
	620	612	605	600	588	576	560
	0. 15	0. 30	0. 55	0. 64	0. 68	0. 70	0. 71
	5486	4300	3136	1663	3210	2642	2411
SCN	1382	2016	1926	1231	2349	2139	2019
	540	532	520	498	482	470	464
	0. 17	0. 39	0. 54	0. 63	0. 68	0. 77	0. 80
	3218	1978	1087	3711	2122	2800	1980
SSCN	1002	1036	862	2662	1644	2162	1620
	526	524	511	502	480	472	460
	0. 18	0. 35	0. 61	0. 67	0. 71	0. 73	0. 76

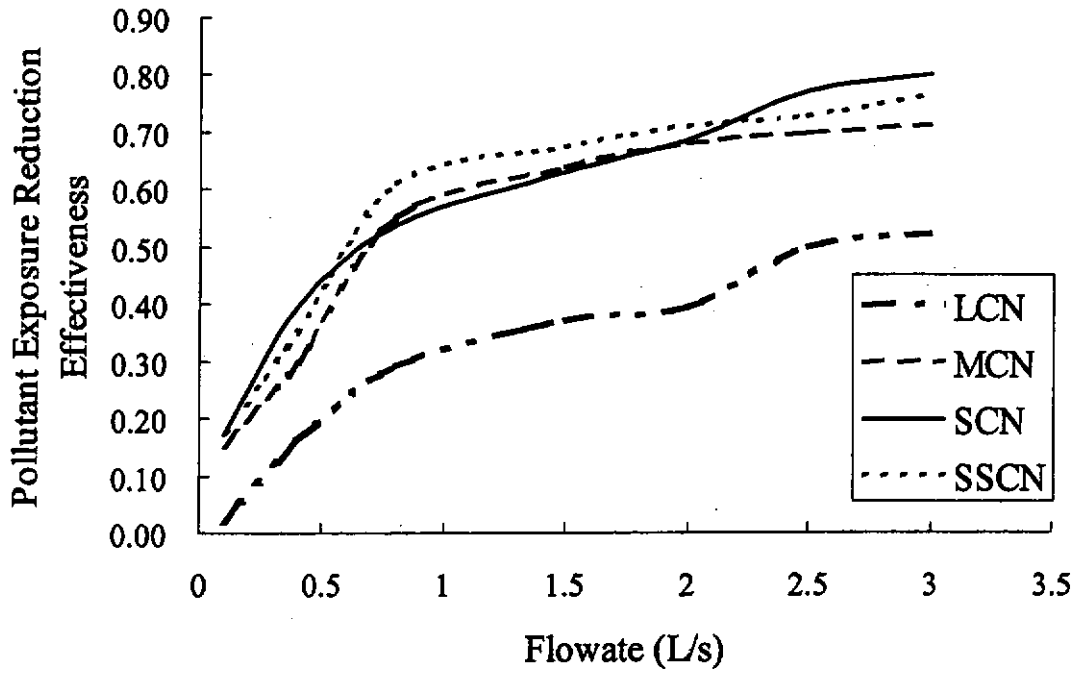

Figure 4.9 Pollutant exposure reduction effectiveness as a function of the airflow rate fromcircular air terminal device: Non-isothermal conditions: room air temperature 22 ℃, personalized air temperature 20℃, the skin temperature of thermal manikin 31℃. LSCN (Large size circular nozzle), MSCN (Middle size circular nozzle), SCN (the small size circular nozzle), SSCN (the smallest circular nozzle)

The cross section of air terminal device LCN, MCN, SCN and SSCN are circular. The diameter of LCN is 12cm. The diameter of MCN is 10cm. The diameter of SCN is 8cm and the diameter of SSCN was 6cm. The results in figure show that the maximum pollutant exposure reduction effectiveness was reached by LCN at 3 L/s, was 0.52. The maximum pollutant exposure reduction effectiveness was reached by MCN at 3 L/s, was 0.71. The maximum pollutant exposure reduction effectiveness was reached by SCN at 3 L/s, was 0.80. And the maximum pollutant exposure reduction effectiveness was reached by SSCN at 3 L/s, was 0.76.

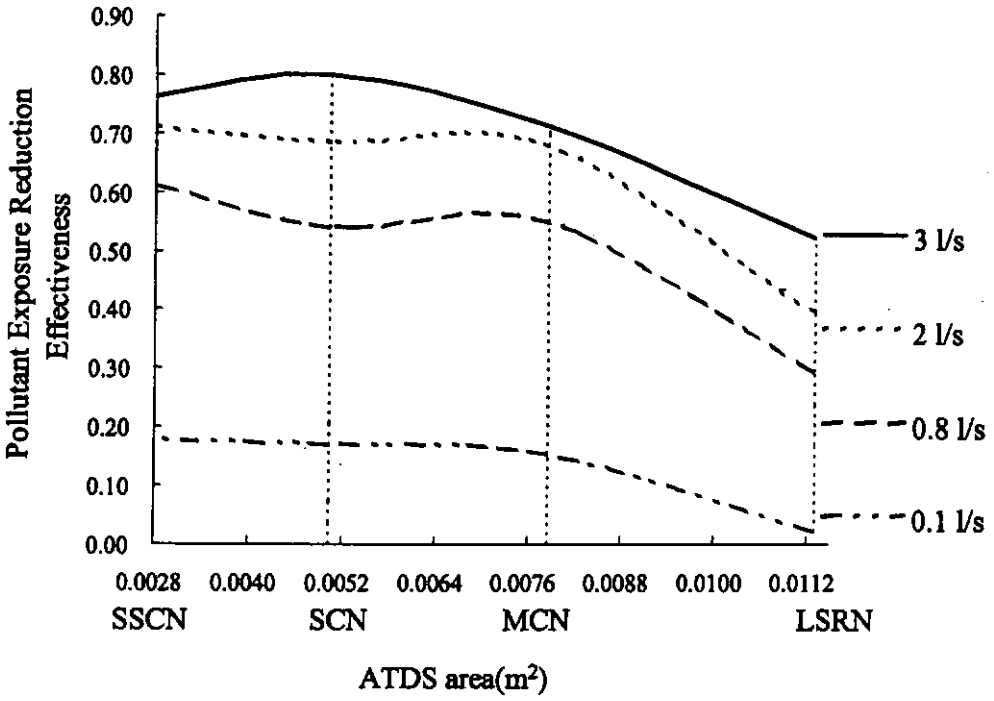

Figure 4.10 Pollutant exposure reduction effectiveness as a function of the area of circular air terminal device: Non-isothermal conditions: room air temperature 22℃, personalized air temperature 20℃, the skin temperature of thermal manikin 31℃. LCN (the large size circular nozzle), MCN (the middle size circular nozzle), SCN (the small size circular nozzle), SSCN (the smallest size circular nozzle)

As shown on Figure 4.10, It is similar to rectangular ATDs, the pollutant exposure reduction effectiveness is also different as the difference of ATDs' cross area at the same airflow rate in circular ATDs. The increasing of cross-area will help to increasing of pollutant exposure reduction effectiveness in initial period as the airflow rate was fixed. The extreme value reached at a certain middle area with certain airflow rate. After this area, the pollutant exposure reduction effectiveness will decrease as the increasing of ATDs' cross-area. In our experiments, for supply airflow rate at 3 l/s, the maximum pollutant exposure reduction effectiveness was reached by SCN at 0.80.

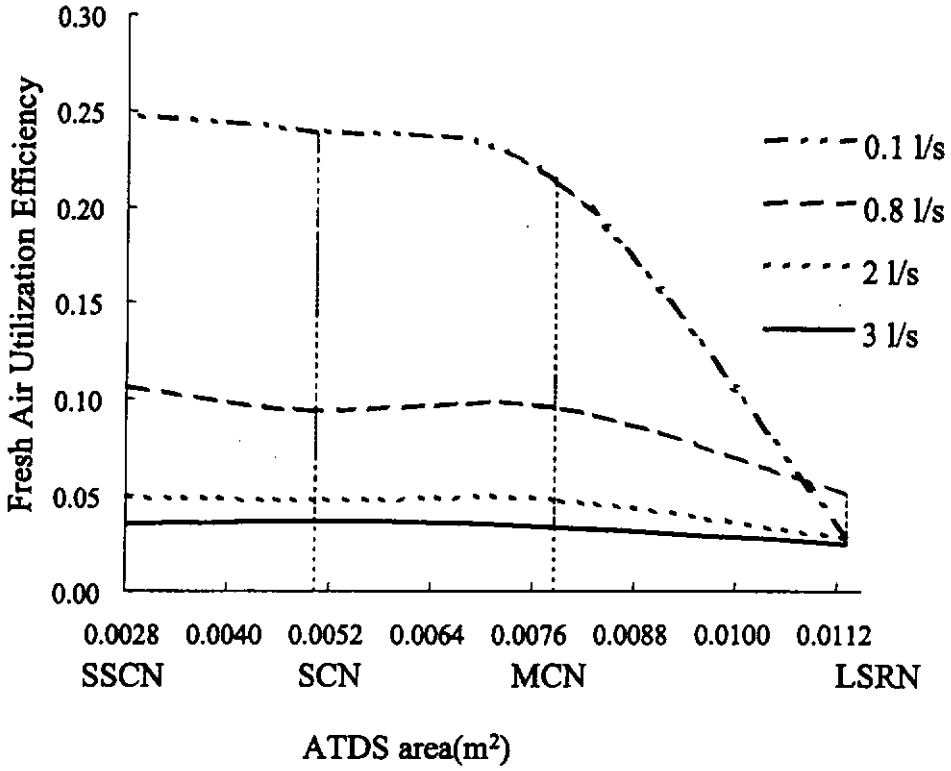

Figure 4.11 Fresh air utilization efficiency as a function of the area of circular air terminal device: Non-isothermal conditions: room air temperature 22℃, personalized air temperature 20℃, the skin temperature of thermal manikin 31℃. LCN (the large size circular nozzle), MCN (the middle size circular nozzle), SCN (the small size circular nozzle), SSCN (the smallest size circular nozzle)

As shown on Figure 4.11, the fresh air utilization efficiency is also different as the difference of ATDs' cross-area at the same airflow rate. Opposite to the pollutant exposure reduction effectiveness, the increasing of cross-area will decrease the fresh air utilization efficiency. The obvious difference of fresh air utilization in different type of ATDs is exit when the airflow rate is 0.1 l/s. As the increasing of airflow rate, this difference becomes more and more unobvious. As the airflow rate equal to 3.0 l/s, the slope almost become flat, or in other words, the cross-area of ATDs will not affect the fresh air utilization efficiency.

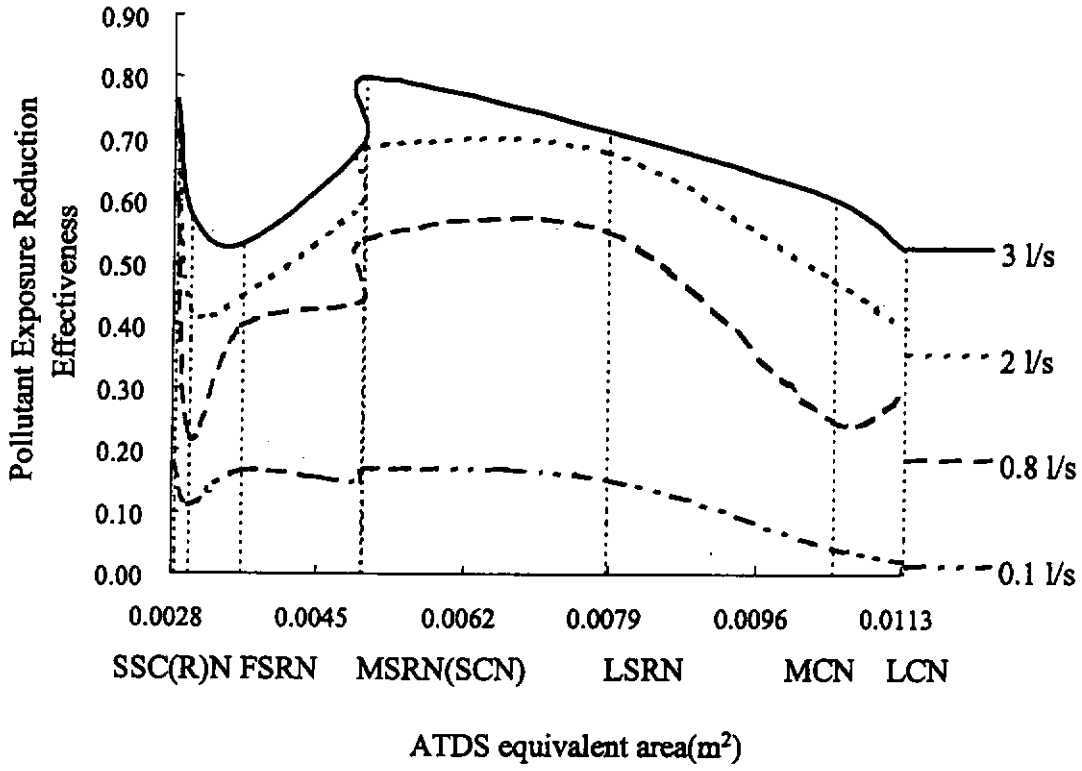

Figure 4.12 Pollutant exposure reduction effectiveness as a function of the cross-sectional area of air terminal device: Non-isothermal conditions: room air temperature 22℃, personalized air temperature 20℃, the skin temperature of thermal manikin 31 ℃. LCN (the large size circular nozzle), MCN (the middle size circular nozzle), SCN (the small size circular nozzle), SSCN (the smallest size circular nozzle), LSRN (the largest rectangular nozzle), MSRN (the middle size rectangular nozzle), SSRN (the small size rectangular nozzle), FSRN (the flat rectangular nozzle)

Figure 4.13 Fresh air utilization efficiency as a function of the cross-sectional area of air terminal device: Non-isothermal conditions: room air temperature 22℃, personalized air temperature 20℃, the skin temperature of thermal manikin 31℃. LCN (the large size circular nozzle), MCN (the middle size circular nozzle), SCN (the small size circular nozzle), SSCN (the smallest size circular nozzle), LSRN (the largest rectangular nozzle), MSRN (the middle size rectangular nozzle), SSRN (the small size rectangular nozzle), FSRN (the flat rectangular nozzle)

Using the concept of hydrodynamic radius,

$$R = \frac{A}{x} = \frac{ab}{2(a+b)} \tag{4-5}$$

where R is the hydrodynamic radius

A is the cross-sectional area

x is the wetted perimeter

a, b are the lengths of rectangular sides

Thus, the cross-sectional area of rectangular ATDs could be converted into equivalent area.

Table 4.10 the equivalent sectional area

SSRN	FSRN	SSCN	MSRN	SCN	LSRN	MCN	LCN
0. 0017	0. 0018	0. 0028	0. 0035	0. 0050	0. 0072	0. 0079	0. 0113

The pollutant exposure reduction effectiveness and fresh air utilization efficiency as a function of equivalent area curve are illustrated in Figure 4.15 and 4.15.

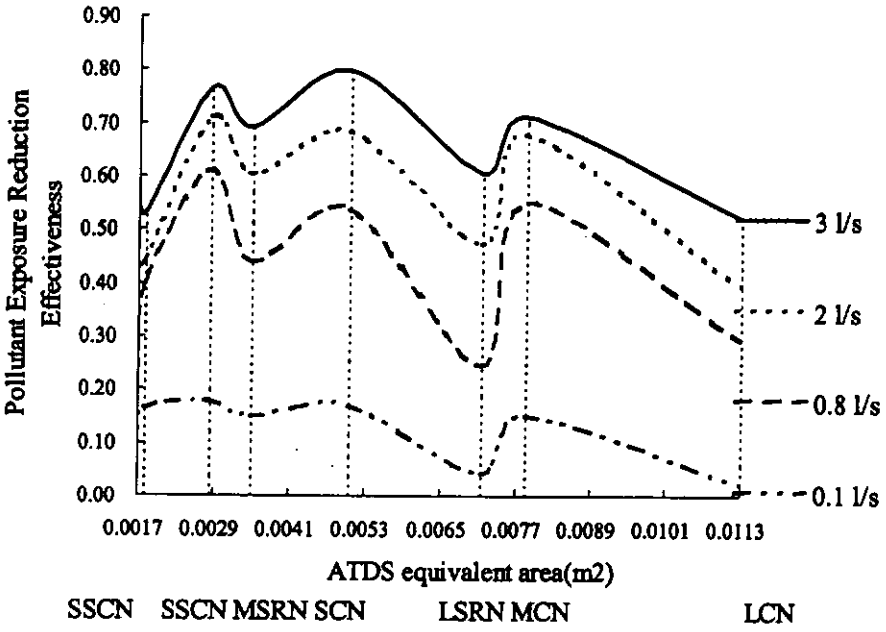

Figure 4.14 Pollutant exposure reduction effectiveness as a function of the equivalent area of air terminal device: Non-isothermal conditions: room air temperature 22℃, personalized air temperature 20℃, the skin temperature of thermal manikin 31℃. LCN (the large size circular nozzle), MCN (the middle size circular nozzle), SCN (the small size circular nozzle), SSCN (the smallest size circular nozzle), LSRN (the largest rectangular nozzle), MSRN (the middle size rectangular nozzle), SSRN (the small size rectangular nozzle), FSRN (the flat rectangular nozzle)

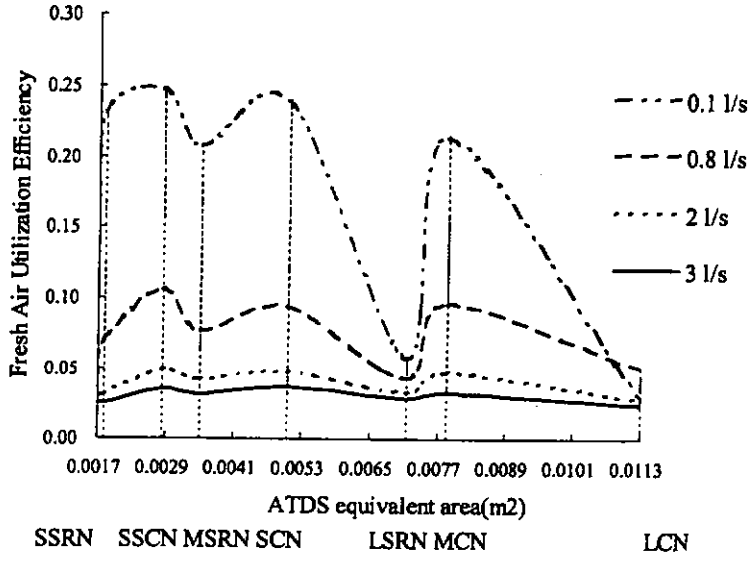

Figure 4.15 Fresh air utilization efficiency as a function of the equivalent area of air terminal device: Non-isothermal conditions: room air temperature 22℃, personalized air temperature 20℃, the skin temperature of thermal manikin 31℃. LCN (the large size circular nozzle), MCN (the middle size circular nozzle), SCN (the small size circular nozzle), SSCN (the smallest size circular nozzle), LSRN (the largest rectangular nozzle), MSRN (the middle size rectangular nozzle), SSRN (the small size rectangular nozzle), FSRN (the flat rectangular nozzle)

As shown on Figure 4.14, As the equivalent area of ATDs increases, the pollutant exposure reduction effectiveness was increasing at first, reaching the maximum values at certain equivalent area value and then starting to decrease. The particularly low η_{PER} values were found for the large size rectangular nozzles. This may be because of the effects of the geometry of a particular ATD, which will be discussed at the following section.

4.4 The effect of nozzle geometry

4.4.1 The effect of proportion between long side and short side of rectangular ATDs

Three series of rectangular ATDs MSRN, SSRN and FSRN were studied to investigate the effect of proportion between long side and short side of rectangular ATDs. The cross section of air terminal device MSRN, SSRN and FSRN were all rectangular. The FSRN has the same cross-sectional area with air terminal device MSRN but different proportion between the long side and the short side.

Table 4.11 The C_f, C_a, C_L and η_f of three series rectangular nozzles (The middle size nozzle, the small nozzle and the flat nozzle)

Flowrate	L/s	0.1	0.4	0.8	1.5	2	2.5	3
	C_f (ppm)	4032	2466	4586	3101	2570	2195	1808
MSRN	C_L (ppm)	1125	1335	2356	1871	1787	1665	1429
	C_a (ppm)	620	618	612	607	602	591	580
	η_f	0.15	0.39	0.44	0.51	0.60	0.67	0.69
	C_f (ppm)	4531	3542	2583	3403	2487	1930	1690
SSRN	C_L (ppm)	1097	1195	1088	1640	1427	1331	1242
	C_a (ppm)	680	680	662	653	640	633	621
	η_f	0.11	0.18	0.22	0.36	0.43	0.54	0.58
	C_f (ppm)	4178	2647	2516	3269	2792	2039	1818
FSRN	C_L (ppm)	1778	1594	1562	1828	1600	1265	1191
	C_a (ppm)	1302	1100	930	790	650	480	480
	η_f	0.17	0.32	0.40	0.42	0.44	0.50	0.53

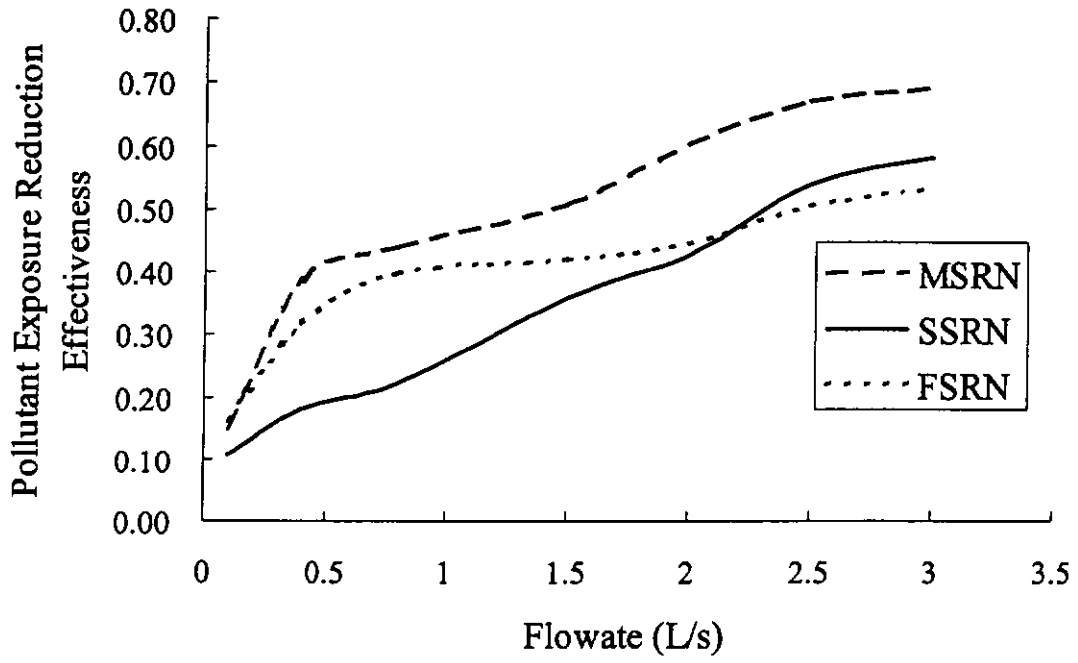

Figure 4.16 Pollutant exposure reduction effectiveness as a function of the airflow rate from air terminal device: Non-isothermal conditions: room air temperature 22℃, personalized air temperature 20℃, the skin temperature of thermal manikin 31℃. MSRN (the middle size rectangular nozzle), SSRN (the small size rectangular nozzle), FSRN (the flat rectangular nozzle)

The results in figure 4.16 show that the slope of the SSRN curve becomes flat at about 3 L/s, the slope of the FSRN becomes flat at about 3 L/s, and the slope of the MSRN becomes flat at about 2.5 L/s. The maximum pollutant exposure reduction effectiveness was reached by SSRN was 0.58, for the FSRN, was 0.53 and for MSRN was 0.69.

The length of long side of SSRN was the same as that of MSRN. But the length of short side was shorter than that of MSRN. It could be concluded that for the middle size air terminal devices, decreasing the length of short side of air terminal device could not increase the pollutant exposure reduction effectiveness. The length of short side of FSRN was the same as that of SSRN, but the length of long side of FSRN was longer than that of SSRN. It could be concluded that, for the small size air terminal devices, increasing the length of long side of air terminal could not increase the pollutant exposure reduction effectiveness. The proportion between the long side and the short side of FSRN was 1.5 times bigger than the proportion of MSRN. It could be concluded that, for middle size air terminal devices, increasing the proportion between the long side and the short side could not increase the pollutant exposure reduction effectiveness. Combined with the discussion before, a conclusion can be drawn that the maximum pollutant exposure reduction effectiveness of ATDs was reached at the appropriate effective area and proportion between the length of long side and the short side. In the series of rectangular ATDs studied, the MSRN with 10cm length and 5cm width appeared to be the optimal one to give the best effectiveness of personal ventilation. For a better comparison of two nozzles of the same area but different geometry, the tested results are presented in bar-chart from Figure 4.17 to Figure 4.20.

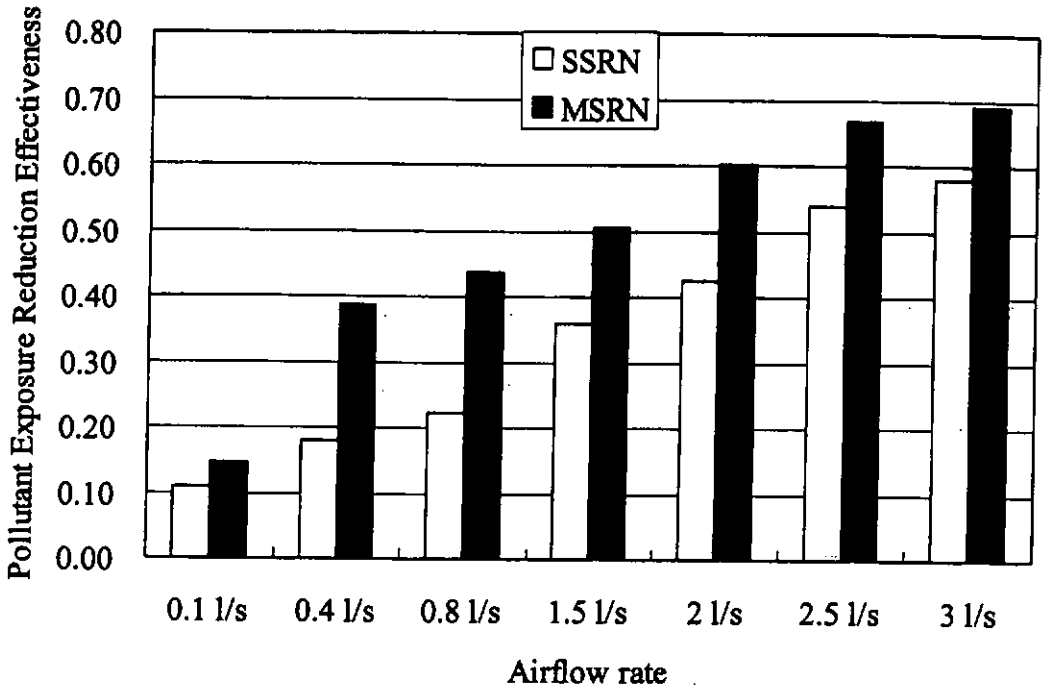

Figure 4.17 Pollutant Exposure Reduction Effectiveness at different length of air terminal device short side as the function of airflow rate: Non-isothermal conditions: room air temperature 22℃, personalized air temperature 20℃, the skin temperature of thermal manikin 31℃. MSRN (the rectangular ATD with the 10cm length in long side and 5cm in short side), SSRN (the rectangular ATD with the 10cm length in long side and 3cm in short side)

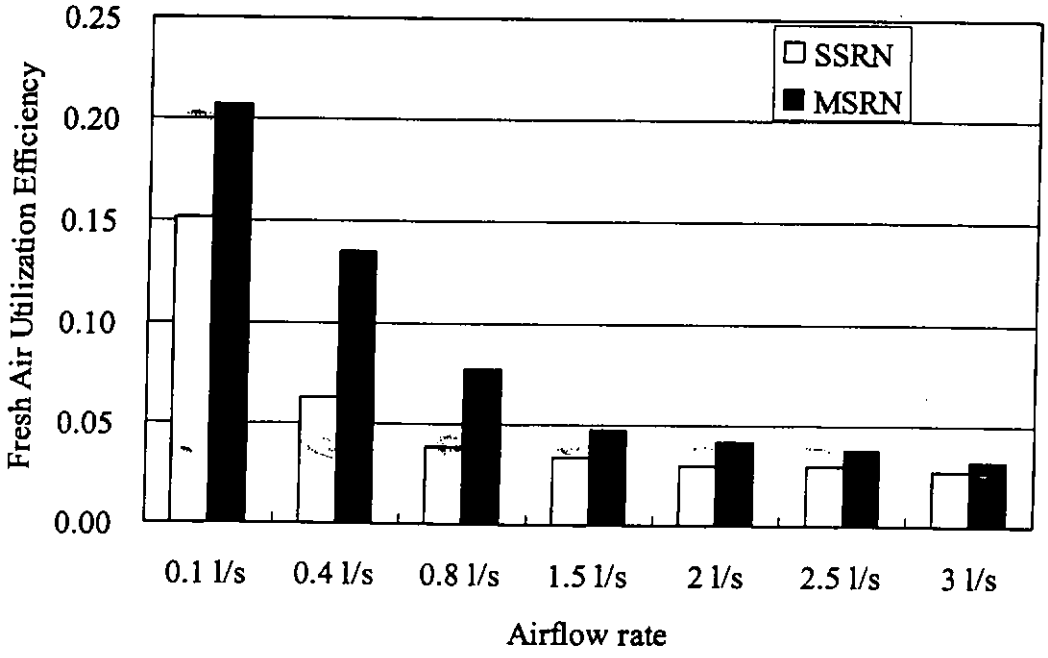

Figure 4.18 Fresh air utilization efficiency at different length of air terminal device short side as the function of airflow rate: Non-isothermal conditions: room air temperature 22℃, personalized air temperature 20℃, the skin temperature of thermal manikin 31℃. MSRN (the rectangular ATD with the 10cm length in long side and 5cm in short side), SSRN (the rectangular ATD with the 10cm length in long side and 3cm in short side)

As shown on Figure 4.17 and Figure 4.18, at certain area of rectangular ATDs, increasing the length of the short side will enhance the effect of personalized air inhaled air quality and fresh air utilization efficiency. This impact is less obvious at the higher airflow rates.

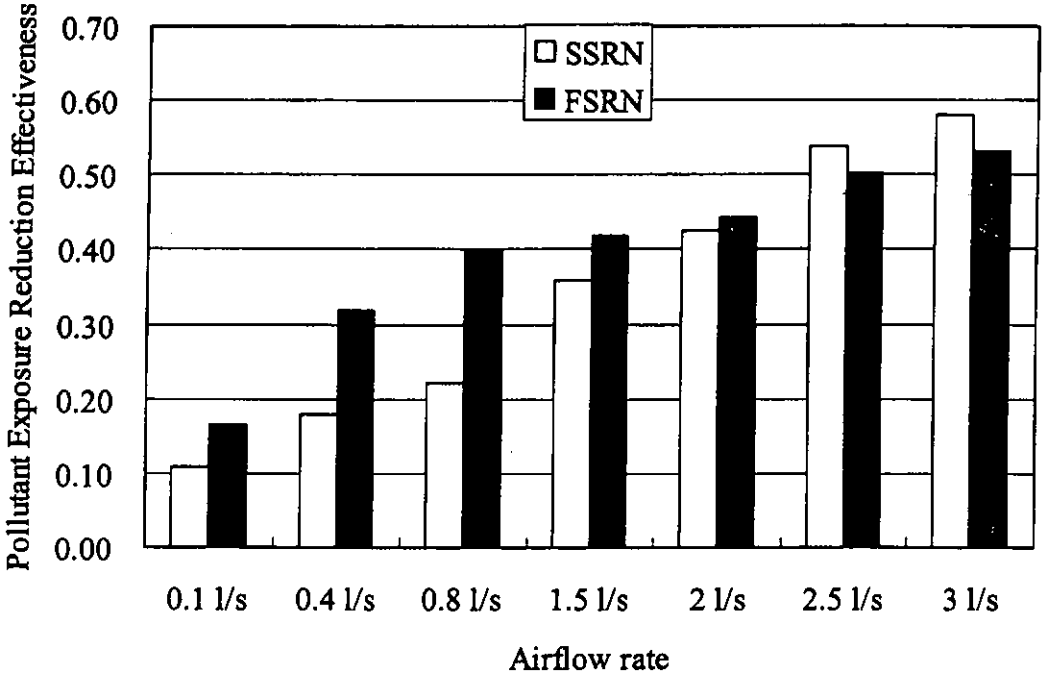

Figure 4.19 Pollutant Exposure Reduction Effectiveness at different length of air terminal device long side as the function of airflow rate: Non-isothermal conditions: room air temperature 22℃, personalized air temperature 20℃, the skin temperature of thermal manikin 31℃. FSRN (the rectangular ATD with the 12cm length in long side and 3cm in short side), SSRN (the rectangular ATD with the 10cm length in long side and 3cm in short side)

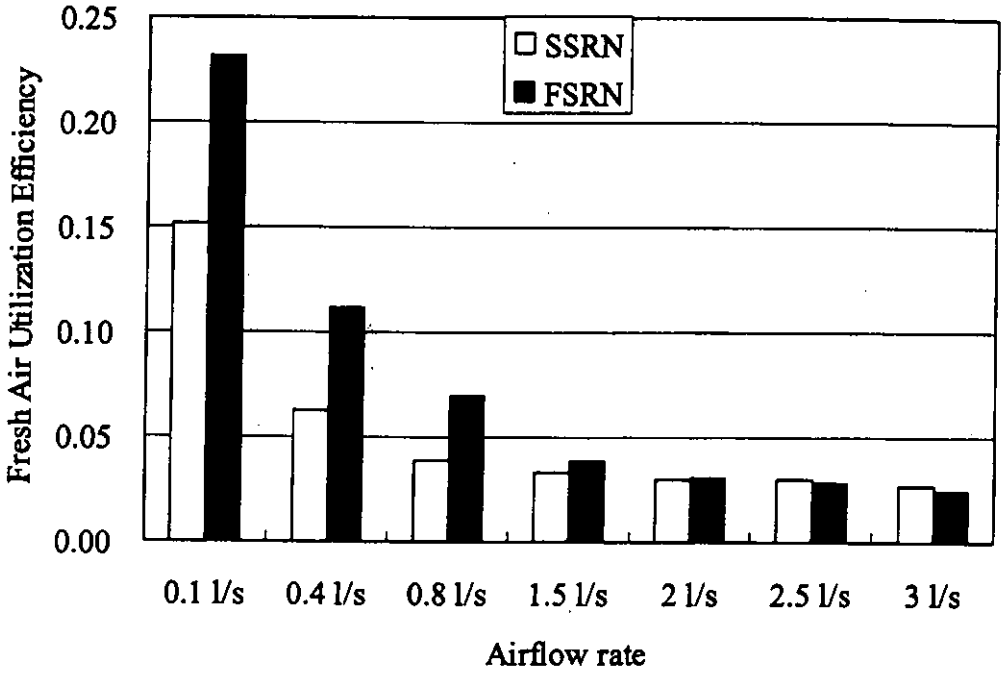

Figure 4.20 Fresh air utilization efficiency at different length of air terminal device long side as the function of airflow rate: Non-isothermal conditions: room air temperature 22℃, personalized air temperature 20℃, the skin temperature of thermal manikin 31℃. FSRN (the rectangular ATD with the 12cm length in long side and 3cm in short side), SSRN (the rectangular ATD with the 10cm length in long side and 3cm in short side)

As shown on Figure 4.19 and Figure 4.20, at certain area of rectangular ATDs, increasing the length of the long side will enhance inhaled air quality and fresh air utilization efficiency at the lower airflow rates between 0.1 to 1.5 l/s, whereas, at higher airflow rates, increasing the length of the long side of rectangular ATDs will reduce the exposure reduction effectiveness and fresh air utilization efficiency.

4.4.2 the effect of shapes of ATDs

Three groups of rectangular ATDs and circular ATDs with same cross-sectional area were studied in this section to investigate the effect of ATDs' shape on inhaled air quality and fresh air utilization efficiency.

Table 4.12 The C_f, C_a, C_L and η_f of two largest nozzles (rectangular nozzle and circular nozzle)

flowrate		LSRN				LCN		
l/s	C_f(ppm)	C_L (ppm)	C_a (ppm)	η_f	C_f(ppm)	C_L (ppm)	C_a (ppm)	η_f
0. 1	4725	783	613	0. 04	4837	670	580	0. 02
0. 4	1913	902	610	0. 22	3116	1004	600	0. 16
0. 8	3549	1329	605	0. 25	4672	1799	614	0. 29
1. 5	2763	1444	600	0. 39	2840	1463	650	0. 37
2. 0	2317	1409	594	0. 47	2623	1429	650	0. 39
2. 5	1983	1370	580	0. 56	2213	1432	657	0. 50
3. 0	1719	1260	560	0. 60	1897	1307	660	0. 52
4. 0	3026	2040	560	0. 60	2982	1850	560	0. 53

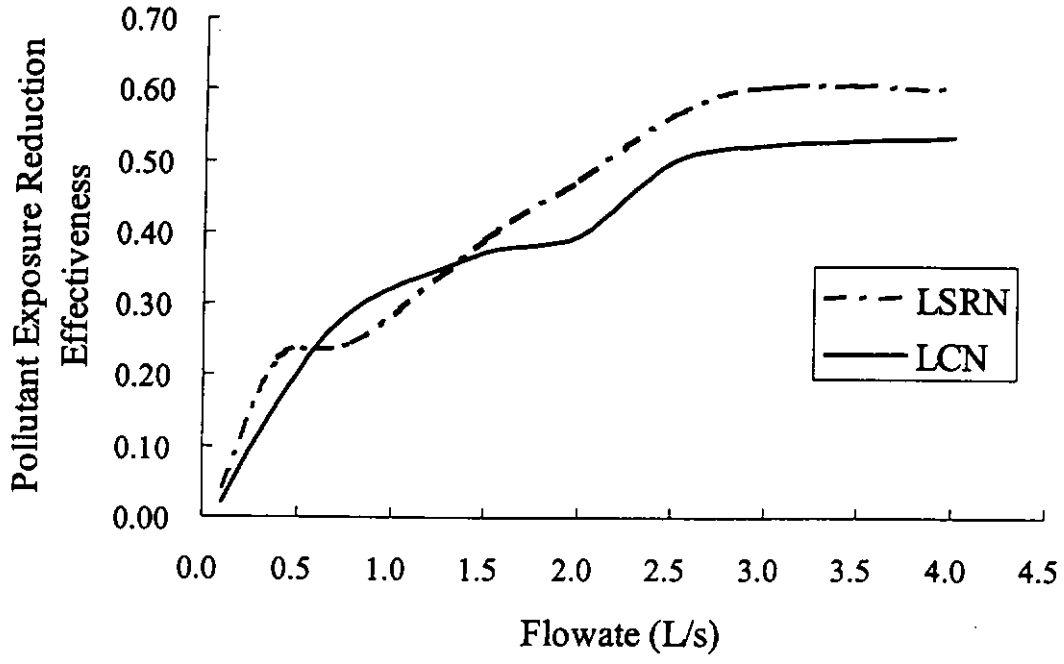

Figure 4.21 Pollutant exposure reduction effectiveness as a function of the airflow rate from air terminal device: Non-isothermal conditions: room air temperature 22℃, personalized air temperature 20℃, the skin temperature of thermal manikin 31℃. LSRN (the largest rectangular nozzle), LCN(the largest circular nozzle)

The air terminal devices LSRN and LCN are the largest air terminal devices of all ATDs in our studies. They have same cross-sectional area, the cross section of LSRN

is rectangular and the LCN is circular. The results in Figure 4.21 show that the slope of the LSRN curve becomes flat at about 3 L/s, and the slope of the LCN becomes flat at about 2.5 L/s. The maximum pollutant exposure reduction effectiveness reached with LSRN was 0.6, and with the LCN, was 0.53. It could be concluded that for the large area of cross section, the rectangular air terminal device is better than circular air terminal device.

Table 4.13 The C_f, C_a, C_L and η_f of two middle air terminal devices with same cross-sectional area (The middle size rectangular nozzle, the small circular nozzle)

flowrate		MSRN				SCN		
l/s	C_f(ppm)	C_L(ppm)	C_a(ppm)	η_f	C_f(ppm)	C_L(ppm)	C_a(ppm)	η_f
0.1	4032	1125	620	0.15	5486	1382	540	0.17
0.4	2466	1335	618	0.39	4300	2016	532	0.39
0.8	4586	2356	612	0.44	3136	1926	520	0.54
1.5	3101	1871	607	0.51	1663	1231	498	0.63
2.0	2570	1787	602	0.60	3210	2349	482	0.68
2.5	2195	1665	591	0.67	2642	2139	470	0.77
3.0	1808	1429	580	0.69	2411	2019	464	0.80
4.0	3450	2540	560	0.69	3078	2585	564	0.80

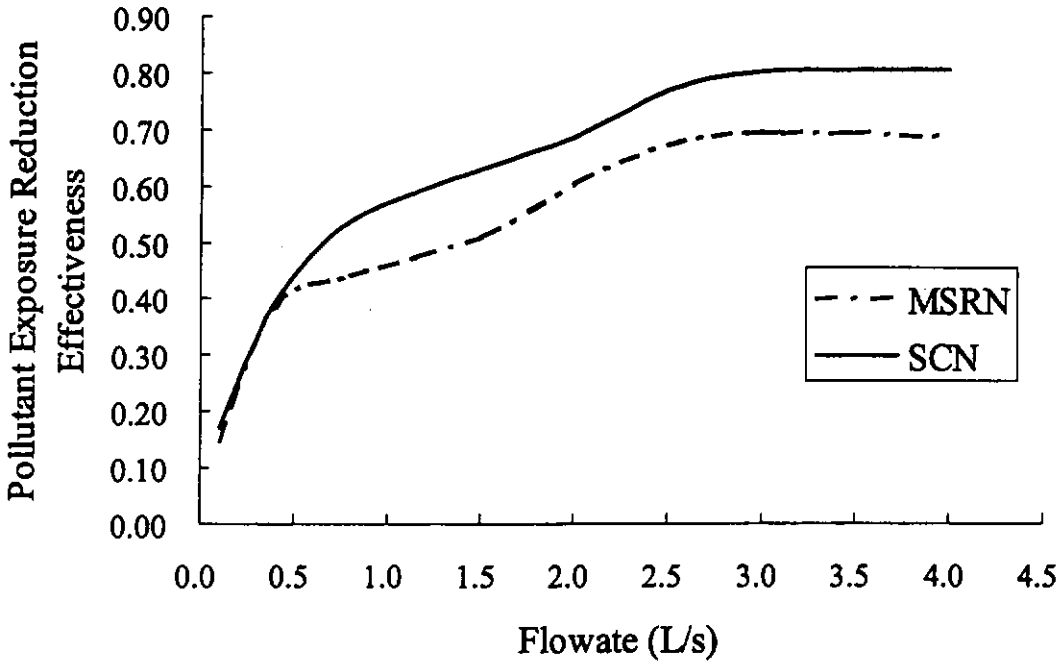

Figure 4.22 Pollutant exposure reduction effectiveness as a function of the airflow rate from air terminal device: Non-isothermal conditions: room air temperature 22℃, personalized air temperature 20℃, the skin temperature of thermal manikin 31℃. MSRN (the middle size rectangular nozzle), SCN (the small size circular nozzle)

The air terminal device SCN has the same cross-sectional area as MSRN. The cross section of SCN was circular. The cross section of MSRN was rectangular. The results in Figure 4.22 show that slope of SCN curve becomes flat at about 3 L/s, and the slope of the MSRN becomes flat at about 2.5 L/s. The maximum pollutant exposure reduction effectiveness reached with SCN was 0.8, for MSRN was 0.69. It could be concluded that for the middle size area of cross section, the circular air terminal device is better than rectangular air terminal device.

Table 4.14 The C_f, C_a, C_L and η_f of two nozzles with close cross-sectional area (The small size rectangular nozzle, the smallest size circular nozzle)

flowrate		SSRN				SSCN		
l/s	C_f(ppm)	C_L(ppm)	C_a(ppm)	η_f	C_f(ppm)	C_L(ppm)	C_a(ppm)	η_f
0.1	4531	1097	680	0.11	3218	1002	526	0.18
0.4	3542	1195	680	0.18	1978	1036	524	0.35
0.8	2583	1088	662	0.22	1087	862	511	0.61
1.5	3403	1640	653	0.36	3711	2662	502	0.67
2.0	2487	1427	640	0.43	2122	1644	480	0.71
2.5	1930	1331	633	0.54	2800	2162	472	0.73
3.0	1690	1242	621	0.58	1980	1620	460	0.76
4.0	1469	1107	611	0.58	1820	1492	460	0.76

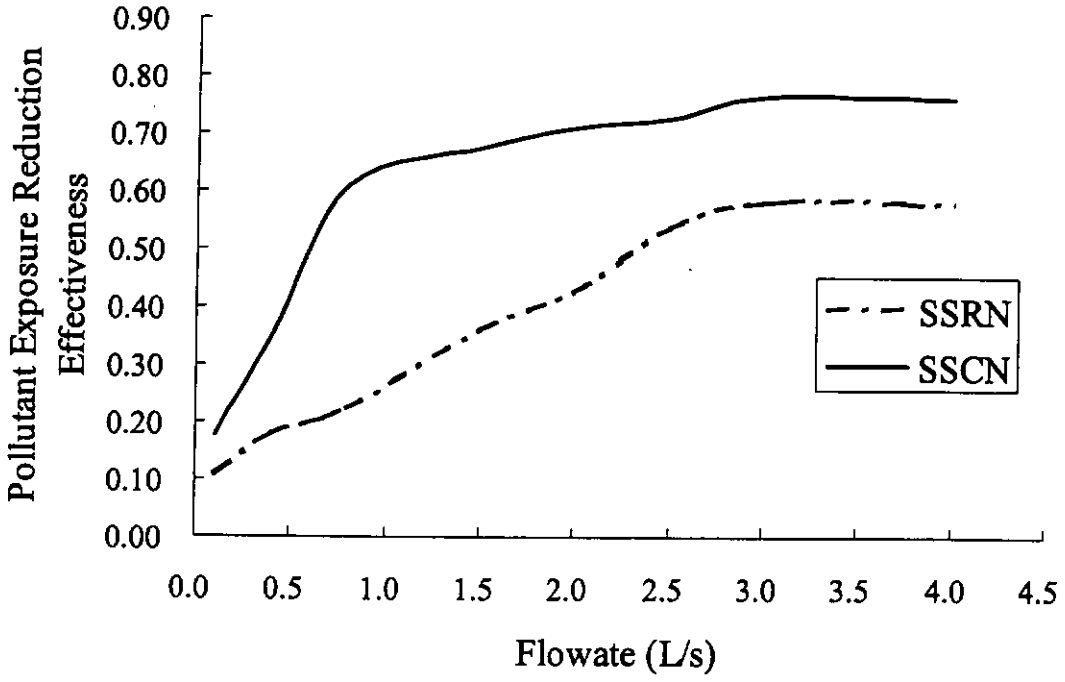

Figure 4.23 Pollutant exposure reduction effectiveness as a function of the airflow rate from air terminal device: Non-isothermal conditions: room air temperature 22℃, personalized air temperature 20℃, the skin temperature of thermal manikin 31℃. SSRN (the small size rectangular nozzle), SSCN (the smallest size circular nozzle)

The air terminal device SSCN has the same cross-sectional area as SSRN. The cross section of SSCN was circular. The cross section of SSRN was rectangular. The results in Figure 4.23 show that the slope of SSCN curve becomes flat at about 2.5 L/s, and

the slope of the SSRN becomes flat at about 3.0 L/s. The maximum pollutant exposure reduction effectiveness reached with SSCN was 0.76, for SSRN was 0.58. It could be concluded that for the small size area of cross section, the circular air terminal device is much better than rectangular air terminal device.

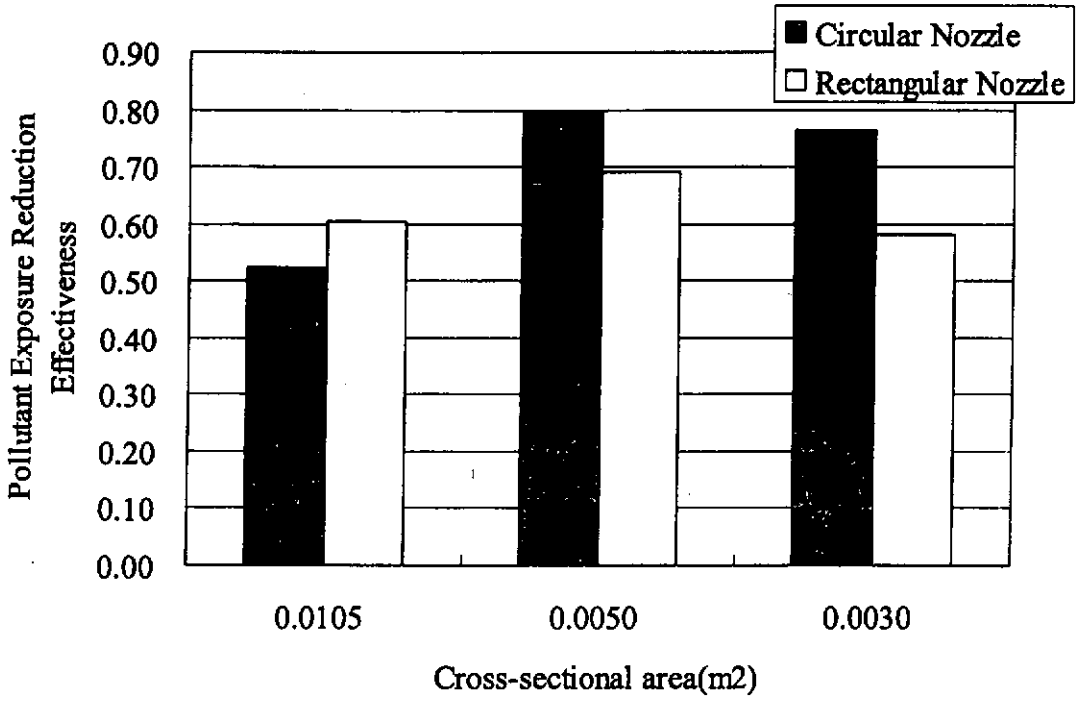

Figure 4.24 Pollutant exposure reduction effectiveness at different cross-sectional area of air terminal device: Non-isothermal conditions: room air temperature 22℃, personalized air temperature 20℃, the skin temperature of thermal manikin 31℃. Airflow rate 3 l/s.

As shown in Figure 4.24, for the circular and rectangular nozzle, the effect of ATDs' shape on pollutant exposure reduction effectiveness was obvious. At fixed airflow rate of 3 L/s, this effect was different at different cross-sectional areas. For the large cross-sectional area, the rectangular nozzle is better than circular nozzle. Whereas, for the middle size, the circular nozzle is better than rectangular nozzle, and for small size, the circular nozzle is much better than rectangular nozzle.

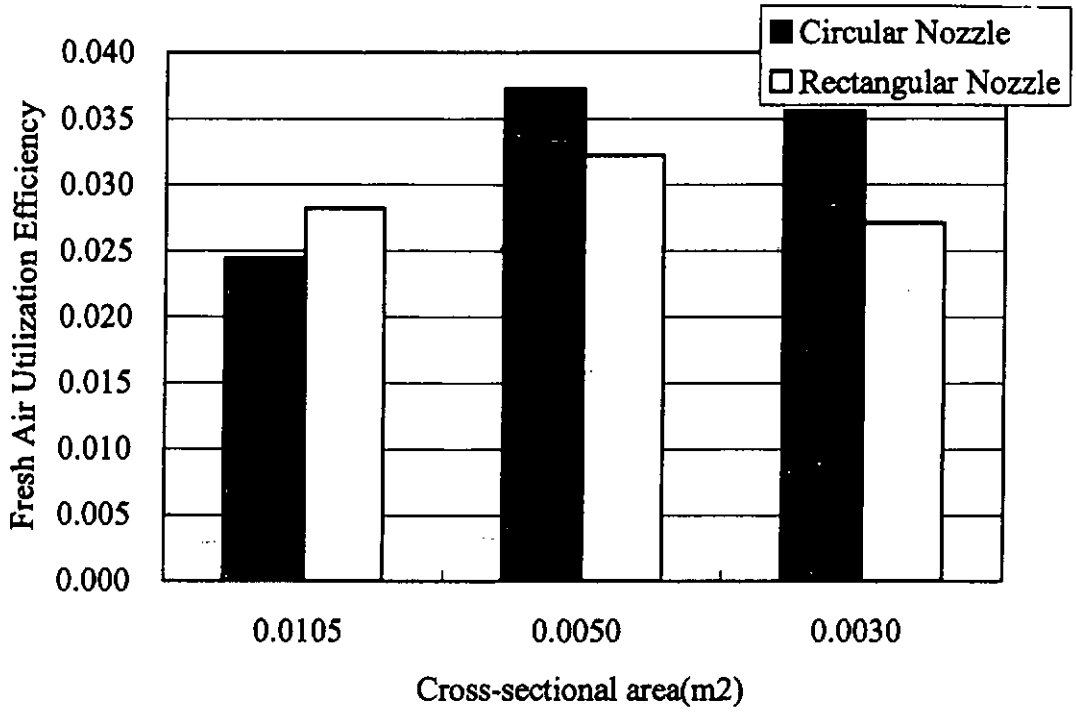

Figure 4.25 Fresh air utilization efficiency at different cross-sectional area of air terminal device: Non-isothermal conditions: room air temperature 22℃, personalized air temperature 20℃, the skin temperature of thermal manikin 31℃. Airflow rate 3 l/s.

As shown on Figure 4.25, for the circular and rectangular nozzle, the effect of ATDs' figure on fresh air utilization efficiency was the same as effect on pollutant exposure reduction effectiveness. At fixed airflow rate, this effect was different at different cross-sectional area. For the large cross-sectional area, the rectangular nozzle is better than circular nozzle. Whereas, for the middle size, the circular nozzle is better than rectangular nozzle, and for small size, the circular nozzle is much better than rectangular nozzle.

4.5 Mixing process analysis of microclimate in the breathing zone

The personalized ventilation air, though directly supplied to the breathing zone, is still contaminated by the ambient air caused by induced mixing. Furthermore, occupant's breathing generates an air movement due to exhalation and inhalation. The interaction between the airflow from the personalized ventilation, the free convection flow around the body and the airflow of respiration determines the final performance.

The effects of free convection flow around the body for the occupants' inhaled air quality has been discussed before. In our experiments, as the measurement, the room temperature was about 20℃, the thermal manikin temperature was about 31℃, and the velocity around the human head due to free convection was about 0.2 m/s.

The occupant's respiration process could be divided into two courses: the inhalation process and exhalation process. For the exhalation process, the airflow due to exhalation was on the opposite direction of personalized ventilation. The airflow due to exhalation would directly mix with the core of the supplied airflow. For the inhalation process, the airflow due to inhalation was on the same direction of personalized ventilation. If the air velocity due to inhalation were higher than supplied air, the breathing zone would be contaminated by ambient air caused by inhaled air induction. In this series of experiments, as the measurement, the air velocity due to respiration was about 0.9 m/s.

If the personalized ventilation flow rate is lower, such as 0.1 L/s to 1.0 L/s, the exhaled air velocity is much higher than that of the personalized ventilation. The exhaled air and free convection flow around the body will have more effects on inhaled air quality. Thus, the pollutant exposure reduction effectiveness will be low. If the personalized ventilation flow rate is higher, such as 2.0 L/s to 3.0 L/s, the personalized ventilation will be the more important factor for inhaled air quality. At a given flow rate, the larger the cross-sectional area of the air terminal devices, the lower of the supplied air velocity. During the inhalation process, the induced mixing action caused by inhaled air will be in effect. During the exhalation process, the exhaled air will more mixed with supplied air in breathing zone. On the other hand, the cross section of supplied airflow was wide, the induced mixing action between supplied air and ambient air caused by supplied air may not affect the core area. For the small air terminal devices, the supplied air velocity was higher. During the inhalation process, the inhaling process will not affect the inhaled air quality. During the exhalation process, the exhaled air will be less mixed with supplied air in breathing. However, the cross section of the supplied airflow was narrow and supplied air velocity was higher. The induced mixing action between supplied air and ambient air may well affect the pollutant level in the inhaled core air

Thus, an optimal air terminal cross sectional area, with appropriate shape will exist to obtain the best performance in a personalized air ventilation system. This may help explain why the air terminal device MSRN has given the best performance in the airflow ranges tested.

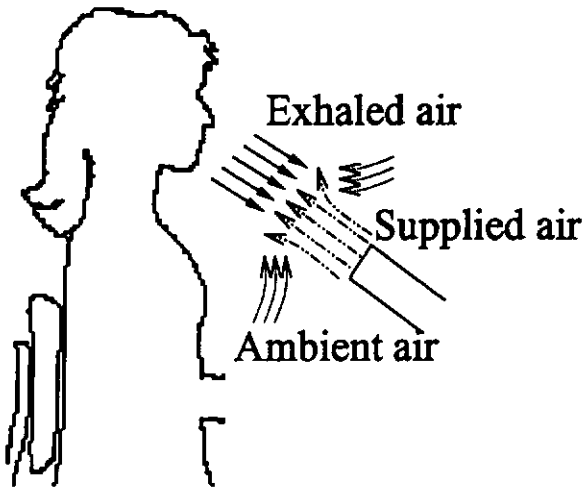

Figure 4.26 The exhalation process of personalized air ventilation

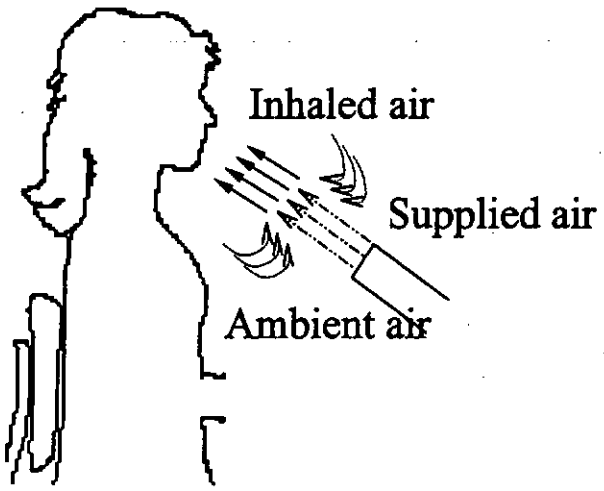

Figure 4.27 The inhalation process of personalized air ventilation

4.6 Conclusions and summery

The inhaled air quality (pollutant exposure reduction effectiveness) and fresh air utilization efficiency was affected by many factors, in these series of experiments, four of them was studied: the airflow around thermal manikin due to heat convection, the supply airflow rate, the cross-sectional area of air terminal devices and the geometry of air terminal devices.

4.6.1 the airflow around thermal manikin due to heat convection

In a calm, comfortable environment, upward free convection movement exists around the human body due to the temperature difference between the room air the surface of the clothing and of the skin of bare body parts. The free convection flow becomes weak when the temperature difference is small. The airflow is slow and laminar with a thin boundary layer at the lower body parts, and fast and turbulent with a thick boundary layer at the height of the head.

The airflow due to heat convection is almost plumb on the supply airflow and airflow due to inhaled or exhaled. It will cut more ambient air in breathing zone. In the series of experiments, the airflow due to heat convection will obviously weak the inhaled air quality and fresh air utilization.

4.6.2 the supply airflow rate

The inhaled air quality will increase due to the increasing the airflow rate. An increase in the flow rate from zero has no immediate effect on the inhaled air quality. Only when a certain initial flow rate is reached does the inhaled air quality for the supply air terminal devices studied start to increase rapidly with the flow rate. It is also clear from the results that the increase in the inhaled air quality due to airflow rate increased could not get 1. It becomes marginal at a certain flow rate until it reaches a steady-state maximum value even if the supply airflow rate increased. The maximum inhaled air quality was found to be different for the different air terminal devices investigated.

On the contrary, the fresh air utilization efficiency decreased due to the increasing the airflow rate. Actually, the fresh air utilization efficiency was very small as an increase in the supply airflow rate from zero. It rapidly reached maximum value in certain initial flow rate and then decreased and becomes marginal at a certain flow rate until it reaches a steady-state minimum value even if the supply airflow rate increased. The maximum fresh air utilization efficiency was found to be different for the different air terminal devices investigated. Whereas, the steady-state minimum value was almost the same for the different air terminal devices investigated.

4.6.3 the cross-sectional area of air terminal devices

In the fixed supply airflow rate, the different cross-sectional area of air terminal devices will produce different supply air velocity and the cross area of supplied air. For different supply air velocity and the area of mixture zone, the mixture process of supply air, inhaled or exhaled air, ambient air due to immixture and cut effect (by airflow due to heat convection through human body) was very complicated. Small cross-sectional area will cause high supply air velocity but small section area of supplied air. This will weaken the cut effect by airflow due to heat convection and the mixture of exhaled air and supplied air in exhalation process, but will strengthen the mixture of ambient air and supplied air due to immixture. Large cross-sectional area will cause low supply air velocity but large section area of supplied air jet. This will weaken the mixing between the ambient air and supplied air, but will strengthen the mixing between the exhaled air and supplied air in the exhalation cycle.

In this series of experiment, in the supply airflow rate range investigated, certain middle size cross-sectional area of air terminal devices achieved good effects in inhaled air quality and fresh air utilization efficiency.

4.6.4 the geometry of air terminal devices

At a fixed supply airflow rate, the geometry of air terminal devices will also affect the inhaled air quality and fresh air utilization efficiency.

For the rectangular air terminal devices, increasing the length of short side of rectangle will increase the inhaled air quality and fresh air utilization. This increasing was obvious in low supply airflow rate. As the supply airflow rate increases further, this effect becomes weakened. Increasing the length of the long side of rectangle will increase the inhaled air quality and fresh air utilization at lower supply airflow rates. at high supply airflow rates, the inhaled air quality and fresh air utilization decrease with the increasing the length of rectangle long side.

At fixed supply airflow rate and fixed cross-sectional area of air terminal devices, at the higher supply airflow rate range, the rectangular air terminal devices is better than circular air terminal devices, whereas, the circular air terminal devices will have better effect on inhaled air quality and fresh air utilization efficiency then the rectangular air terminal devices at the smaller cross-sectional area.

CHAPTER V: CONCLUSION AND RECOMMENDATIONS

5.1 The application potentials

Personalized air supplied to the breathing zone of each individual is a promising concept, allowing a quality of the air for breathing that is optimal for human perception and productivity.

The performance of eight supply air terminal devices (ATD) for a personalized ventilation system was tested in regard to quality of inhaled air and fresh air utilization efficiency. Two new indices, pollutant exposure reduction effectiveness, expressed as the percentage of personalized air in inhaled air, was introduced to assess the performance of the tested air terminal devices. The fresh air utilization efficiency, which expressed the ratio of actual fresh air in the inhaled to the supplied air, was introduced to assess the energy use for the fresh air.

The pollutant exposure reduction and air utilization are still many times higher than the conventional general ventilation system, which indicates that the system can be very promising in those work places where occupants are sitting in a fixed position for prolonged period.

5.2 The optimal air terminal device

The personal exposure reduction effectiveness increased with the increase of the airflow rate from the ATD to a constant maximum value, which was not affected by a further increase of the airflow. The inhaled air quality and fresh air utilization efficiency are affected by many factors: the airflow around thermal manikin due to heat convection, the supply airflow rate, the cross-sectional area of air terminal devices and the geometry of air terminal devices. For the performance of eight supply air terminal devices (ATD) for a personalized ventilation system, the air terminal device SCN does the best performance for the personalized air ventilation system. As the supply method, the air terminal device was directly located on chin position, the maximum pollutant reduction exposure of SCN was reached at 3 L/s, was 0.8. The airflow rate is much lower than that of the desktop supply method tested by Melikov (2001) and the maximum pollutant exposure reduction value is also higher. The supply method adopted in this experiment appears to have a good performance.

5.3 Future works

The interaction between the airflow from the personalized ventilation, the free convection flow around the body and the airflow of respiration are very complicated processes. To investigate the detail interaction between airflow due to heat convection, supply airflow and occupant's inhalation and exhalation in different supply method, to predict the inhaled air quality and fresh air utilization

efficiency, the computational fluid dynamics will be very useful in the future. And in the CFD model, the built-in of the respiration model of occupant will be very important. Also thermal comfort and occupants' acceptability of the personalized air supply should be investigated.

APPENDIX: ANALYSIS OF THE BENEFITS OF THE PERSONAL AIR SUPPLY METHOD

a). The reduced exposure to indoor air pollutants

Assume that the emission rate of indoor pollutants is $\dot{E}$, and the total ventilation rate is Q. With the introduction of personal ventilation (PA) rate Q_P, and the background ventilation is reduced to $Q_B = Q - Q_P$, i.e., the total ventilation rate remains the same as in a conventional design. According the current ventilation standard, Q is typically around 10 liter per second.

Assume a well-mixed condition in the room, the indoor air pollutant level in the room air will be

$$C = C_s + \dot{E}/Q \qquad (A.1)$$

Where, Cs is the pollutant level in the supply air. C would be the pollutant concentration in the inhaled air with the conventional air supply methods.

With the introduction of personalized air supply, concentration pollutant levels in the room will remain the same. The concentration of pollutants in the inhaled air C_{in} becomes

$$C_{in} - Cs = (1 - \eta_{PER})\,(C - Cs) = (1 - \eta_{PER})\,\dot{E}/Q \qquad (A.2)$$

Where, η_{PER} is the pollutant exposure reduction efficiency of the air supply method. According to our test results, η_{PER} ranges from 9 to 61% at the range from 0.1 to 2 liter/second of Q_P. This means that at the same total ventilation rate, 61% of reduction of indoor air pollutants in the inhaled air is achieved when 2 l/s of the total ventilation air is delivered through the personalized air supply nozzle.

b). The reduced total ventilation rate to achieve equivalent inhaled air quality

The benefit of the new air supply method can be alternatively quantified by demonstrating that ventilation rate can be much reduced to achieve the same inhaled air quality.

Let's assume that the total ventilation rate Q is reduced to 4 l/s, and that Q_P, which is 2 l/s, is delivered via the PA nozzle. Let's assume that $\dot{E}$ remains the same, the indoor air pollutant level will be raised due to the reduced ventilation rate according to Equation (A.1), when compared with the case when Q = 10 l/s:

$$C' = Cs + \dot{E}/(0.4\,Q) \qquad (A.3)$$

However, with the PA system, the pollutant concentration according to Equation (A.2) in the inhaled air would be

$$C_{in} - Cs = (1 - \eta_{PER})\,(C' - Cs) = (1 - \eta_{PER})\ \dot{E}/(0.4\ Q) \qquad (A.4)$$

Since η_{PER} is equal to 61 % at the Qp = 2 l/s, from Equation (A.4), we will have

$$C_{in} = Cs + \dot{E}/Q \qquad (A.5)$$

Comparing (A.5) and (A.1), we can see that Cin = C. That is to say, equivalent inhaled air quality is achieved at the total ventilation rate of merely 40% of the conventional system. This means that the PA method can save 40% of ventilation air, which means significant saving of energy used in air-conditioning.

In summary, the benefits of the PA system can be quantified in both improved inhaled air quality and reduced energy use in air-conditioning.

REFERENCES

(1) ASHRAE. "ASHRAE handbook-Fundamentals, chapter 8". American Society of Heating, Refrigerating and Air-Conditioning Engineers, Inc. Atalanta. (1989)

(2) ASHRAE Standard 62, *Ventilation for acceptable indoor air quality.*: American Society of Heating, Refrigerating and Air-Conditioning Engineers. Atlanta (GA) (1999)

(3) Banhidi L, Somogyi S, Fabo L, and Simon T. "Compensation of asymmetric radiation heat loss to cold walls by different heating systems-Analysis with thermal manikin". *Environment International.*Vol 17(4), pp 211-216. (1991)

(4) Bischof, W., and T.L. Madsen. "Physiological adaptation of thermal manikins". Proceedings of International Symposium on Man and Environment System '91. Tokyo, pp. 147-150. (1991)

(5) Bluyssen PM, de Oliveira Fernandes E, Groes L, Clausen G, Fanger PO, Valbjùrn O, et al. "European indoor air quality audit project in 56 office buildings". Indoor Air 1996, Vol 6, pp 221-238. (1996)

(6) Brohus H, Nielsen PV. "Personal exposure to contaminant sources in a uniform velocity field", Healthy Buildings '95. (1995)

(7) Brohus, H., Nielsen, P.V. "Personal Exposure in Displacement Ventilated Rooms". *Indoor Air*, Vol. 6, pp.157-167. (1996)

(8) CEN. *Ventilation for Buildings: Design Criteria for the Indoor Environment.*: European Committee for Standardization (CER 1752), Brussels (1998)

(9) ECA (European Concerted Action ``Indoor Air Quality and its Impact on Man''). "Guidelines for Ventilation Requirements in Buildings". *Report No. 11, EUR 14449*, Office for Official Publications of the European Communities. EN. Luxembourg, (1992)

(10) EN ISO. *Moderate thermal environments - determination of the PMV and PPD indices and specification of the conditions for thermal comfort* (EN ISO Standard 7730). International Organization for Standardization. (1993)

(11) Fang, L., Clausen, G., Fanger, P.O. "Impact of Temperature and Humidity on the Perception of Indoor Air Quality". *Indoor Air*, Vol 8, pp.80-90. (1998)

(12) Fang, L., Clausen, G., Fanger, P.O. "Impact of Temperature and Humidity on Chemical and Sensory Emissions from Buildings Materials". *Indoor Air*, Vol 9, pp.193-201. (1999)

(13) Fanger PO. "Thermal comfort: analysis and applications in environmental engineering". Copenhagen: Danish Technical Press. (1970)

(14) Fanger PO, Ipsen BM, Langkilde G, Olesen BW, Christensen NK, and Tanabe S. 1986. "Comfort limits for asymmetric thermal radiation". *Energy and Buildings*. Vol 8(3), pp. 225-236. (1986)

(15) Fanger PO, Banhidi L, Olesen BW, and Langkilde G. "Comfort limits for asymmetric thermal radiation". *ASHRAE Transactions*. Vol 86(2), pp 141-156. (1980)

(16) Fanger PO. "Human requirements in future air-conditioned environments", International Journal of Refrigeration, Vol 24, pp 148-153. (2001)

(17) Fanger PO, Melikov A, Hanzawa H, Ring J. 1988. "Air turbulence and sensation of draught". *Energy and Buildings*, Vol 12, pp. 21-39. (1998)

(18) Fisk WJ, Mendell MJ, Daisey JM, Faulkner D, Hodgson AT, Macher JM. "The California healthy building study. Phase 1: a summary". Proceedings of Indoor Air '93, vol 1, pp 279-284. (1993)

(19) Huang DY. *Physical Diagnostics*. China Commerce Publishing Co. China. (1977)

(20) Kerslake, Mck D, Clifford JM. "A comparison of the performance of five air-ventilated suited as heated manikin". N67-10546, *Flying Personal Research. London*: Air Force Department, U.K. Ministry of Defense. (1965)

(21) Madsen TL. 1971. "A new Instrument for Measuring Thermal Comfort". *5th International Congress for Heating, Ventilating and Air Conditioning*. Copenhagen, May 1971. (1971)

(22) Madsen TL. "Mesures de Confort Thermique". Chauers de l'Association Francaise de Biometeorologie. Vol. V. No. 4. (1972)

(23) Madsen TL. "Description of a Thermal Manikin for Measuring the Thermal Insulation Values of Clothings". *Report no 48*. Thermal Insulation Laboratory, The Technical University of Denmark. (1976)

(24) Madsen TL. "Thermal comfort measurements". *ASHRAE Transactions*. Vol. 82(1): pp 60-75. (1976b)

(25) Madsen TL, and Olesen BW. "A new Method for Evaluation of the Thermal Environment in Automotive Vehicles". *ASHRAE Transactions*, Vol.92, Part 1B, pp. 38-54. (1986)

(26) McCullough EA, Jones BW, Huck J. "A comprehensive data base for estimating clothing insulation". *ASHRAE Transactions*. Vol 91, pp 29-47. (1985)

(27) Melikov, A.K. and Nielsen, J.B. "Local thermal discomfort due to draft and vertical temperature difference in rooms with displacement ventilation". *ASHRAE Transactions*, Vol.96,pp.1050-1057. (1989)

(28) Melikov, A., Kaczmarczyk, J., Cygan, L. "Indoor Air Quality Assessment by a breathing thermal manikin". *Proceedings of ROOMVENT 2000*, July 9-12 2000, pp. 101-106. Reading, UK. (2000)

(29) Melikov, A., Cermak, R., Mayer, M.. "Personalized ventilation: evalation of different air terminal devices", *Clima 2000/Napoli 2001 World Congress – Napoli (I)* , 15-18 September 2001, Napoli. (2001)

(30) Mendell MJ. "Non-specific symptoms in office workers: a review and summary of the epidemiologic literature". Indoor Air 1993, vol 3, pp 227-236. (1993)

(31) Mihira K, Toda H, and Arai H. "Study on thermal manikin". *Japanese Journal of Human Factors*. Vol 13(2), pp. 47-53. (1977)

(32) Nielsen M, Pedersen L. "Studies on the Heat Loss by Radiation and Convection from the Clothed Human Body", Acta, Phys, Scandinav, Vol. 27, pp 272-294. (1952)

(33) Olesen BW, Scholer M, and Fanger PO. "Discomfort caused by vertical air temperature differences". *In indoor climate*, pp 561-579, Copenhagen: Danish Building Research Institute. (1979)

(34) Olesen BW, and Madsen TL. "Measurement of the Thermal Insulation of Clothings by a movable Thermal Manikin". *Biophysical and Physiological evaluation of Protective Clothing*. L'Institute Textile de France, Lyon, France, July 1983. (1983)

(35) Pejtersen J, Schwab R, Mayer E. "Sensory evaluation of the air in 14 office buildings: part of an interdisciplinary SBS study in Germany". Proceedings of Indoor Air '99, Edinburgh 1999, Vol 5, pp. 390-395. (1999)

(36) Rapp G.M. "Convective Heat Transfer and Convective Coefficients of Nude Man, Cylinders and Spheres at Low Air Velocities". ASHRAE Transaction, No 2264, pp 75-87. (1973)

(37) Tanabe S, Kimura K, and Inoue U. "Proposal of evaluation method with thermal manikin". *Annual Meeting of Architectural Institute of Japan*, pp 875-876. (1989)

(38) Tanabe S, Arens EA, Bauman FS, Zhang H, and Madsen TL. "Evaluating Thermal Environments by using a Thermal Manikin with controlled Skin Surface Temperature". *ASHRAE winter meeting*, 1994, New Orleans, USA. (1994)

(39) Toda K. "Thermal Manikin and its application for clothing study". *Japanese Journal of Hygiene* 13(1): 146. (1958)

(40) Tsuzuki, K., Arens, E.A., Bauman, F.S., Wyon, D.P. "Individual Thermal Comfort Control with Desk-Mounted and Floor-Mounted Task/Ambient Conditioning (TAC) Systems". *Proceedings of Indoor Air' 1999*, Edinburgh, UK. (1999)

(41) Winslow, L.E.A., Herrington LP. *Temperature and human life*, pp 132-144. Princetion, NJ: Princetion University Press. (1949)

(42) Wyon DP, Larsson S, Forsgren B, and Lundgren I.. "Standard procedures for assessing vehicle climate with thermal manikin". *The Engineering Society for Advancing Mobility Land Sea Air and Space* (SAE), pp 1-11. (1989)

(43) Wyon DP, and Sandberg M. "Thermal Manikin prediction of discomfort due to displacement ventilation". *ASHRAE Transactions*. Vol 96(1). (1990)

(44) Zuo, H.G, Niu, J.L. and Chan, W.T.D., Experimental study of facial air supply method for the reduction of pollutant exposure, *Indoor Air 2002 - The Ninth International Conference on Indoor Air Quality and Climate*, Monterey, California, June 30 – July 5, 2002, pp.1090-1095